MIMO Two-Way Relaying: A Space-Division Approach

Xiaojun Yuan, *Member, IEEE*, Tao Yang, *Member, IEEE*, and Iain B. Collings, *Senior Member, IEEE*,

arXiv:1209.3702v1 [cs.IT] 17 Sep 2012

Abstract

We propose a novel space-division based network-coding scheme for multiple-input multiple-output (MIMO) two-way relay channels (TWRCs), in which two multi-antenna users exchange information via a multi-antenna relay. In the proposed scheme, the overall signal space at the relay is divided into two subspaces. In one subspace, the spatial streams of the two users have nearly orthogonal directions, and are completely decoded at the relay. In the other subspace, the signal directions of the two users are nearly parallel, and linear functions of the spatial streams are computed at the relay, following the principle of physical-layer network coding (PNC). Based on the recovered messages and message-functions, the relay generates and forwards network-coded messages to the two users. We show that, at high signal-to-noise ratio (SNR), the proposed scheme achieves the asymptotic sum-rate capacity of MIMO TWRCs within $\frac{1}{2}\log(5/4) \approx 0.161$ bits per user-antenna for any antenna configuration and channel realization. We perform large-system analysis to derive the average sum-rate of the proposed scheme over Rayleigh-fading MIMO TWRCs. We show that the average asymptotic sum-rate gap to the capacity upper bound is at most 0.053 bits per relay-antenna. It is demonstrated that the proposed scheme significantly outperforms the existing schemes.

I. INTRODUCTION

During the past decade, tremendous progress has been made in the field of network coding [1]. In [2]-[4], the concept of physical-layer network coding (PNC) was introduced and applied to wireless networks. The simplest model for wireless PNC is a two-way relay channel (TWRC), in which two users A and B exchange information via an intermediate relay. Compared with conventional schemes, PNC allows the relay to deliver

This manuscript is submitted to IEEE Transactions on Information Theory

linear functions of the users' messages, which can potentially double the network throughput. It has been shown that the PNC scheme can achieve the capacity of a Gaussian TWRC within 1/2 bit per user [5][6], and its gap to the capacity vanishes at high signal-to-noise ratio (SNR).

Recently, efficient communications over MIMO TWRCs have attracted much research interest, where the two users and the relay are equipped with multiple antennas. Most work on MIMO TWRCs focuses on classical relaying strategies borrowed from one-way relay channels, such as amplify-and-forward (AF) [8]-[10], compress-and-forward [11][12], and decode-and-forward (DF) [13]-[15]. These strategies generally perform well away from the channel capacity due to noise amplification and multiplexing loss [15]. Recently, several relaying schemes have been proposed to support PNC in MIMO TWRCs [16]-[19]. The basic idea is to jointly decompose the channel matrices of the two users to create multiple scalar channels, over which multiple PNC streams are transmitted. Let n_A, n_B, and n_R denote the numbers of antennas of user A, user B, and the relay, respectively. For configurations with $n_A, n_B \geq n_R$, a generalized singular-value-decomposition (GSVD) scheme was shown to achieve the asymptotic capacity of MIMO TWRCs at high SNR [16]. For configurations with $n_A, n_B < n_R$, all existing schemes may perform quite far away from the capacity. Such configurations, however, are of most practical importance. For example, due to the constrained physical sizes of the user terminals, it is usually convenient to implement more antennas at the relay station than at the user ends, as suggested in the standards of next generation networks [20][21].

In this paper, we propose a new space-division based PNC scheme for MIMO TWRCs. Specifically, we first establish a novel joint channel decomposition, which characterizes the mutual orthogonality of the channel directions of the two users seen at the relay. Based on this decomposition, the overall signal space is divided into two orthogonal subspaces. In one subspace, the channel directions of one user are orthogonal (or close to orthogonal) to those of the other user. In this subspace, the spatial streams of the two users are completely decoded. In the other subspace, the channel directions of the two users are parallel or close to parallel. In this subspace, linear functions of the corresponding spatial streams are computed, without completely decoding the individual spatial streams. These linear functions of the spatial streams are referred to as *network-coded messages*. The messages and the network-coded messages, respectively generated from the two subspaces, are jointly encoded at the relay, and then forwarded to the two users. Afterwards, the two users recover their desired messages.

We derive the achievable rates of the proposed space-division based PNC scheme for MIMO TWRCs. We analytically show that, in the high SNR regime, the proposed scheme can achieve the sum capacity of the MIMO TWRC within $\min\{n_A, n_B\} \log(5/4)$ bits, or $\frac{1}{2}\log(5/4) \approx 0.161$ bit/user-antenna, for any antenna setup and channel realization. This gap is much smaller than (as low as 10% of) the gap for the existing best scheme. We also perform large-system analysis to derive the average achievable sum-rate of the proposed scheme in Rayleigh fading MIMO TWRCs. We show that, in the high SNR regime, the average gap between our scheme and the sum-capacity upper bound is greatest when the antenna configuration is $n_A = n_B = \frac{1}{2}n_R$, with the gap being only 0.053 bit/relay-antenna. For all other configurations, the proposed scheme perform even closer to the capacity upper bound. Particularly, as the ratio n_A/n_R (or n_B/n_R) tends to 0 or 1, the gap to the capacity upper bound vanishes. All these analytical results agree well with the simulation. Numerical results demonstrate that the proposed scheme significantly outperforms the existing schemes in the literature across the full range of SNRs.

II. PRELIMINARIES

A. Notation

The following notations are used throughout this paper. We use lowercase regular letters for scalars, lowercase bold letters for vectors, and uppercase bold letters for matrices. The superscripts $(\cdot)^T$ and $(\cdot)^\dagger$ denote transpose and Hermitian transpose, respectively. $\|\cdot\|$ and $\|\cdot\|_F$ represent the Euclidian norm of a vector and the Frobenius norm of a matrix, respectively. $\mathcal{C}(\mathbf{X})$ represents the columnspace of a matrix $\mathbf{X}$. $\mathbb{R}^{n\times m}$ and $\mathbb{C}^{n\times m}$ denote the n-by-m dimensional real space and complex space, respectively. The operation $\log(\cdot)$ denotes the logarithm with base 2, and $|\cdot|$ the determinant. $I(i)$ is the indicator function with $I(i) = 1$ for $i = 1$ and $I(i) = 0$ for $i \neq 1$; $[\cdot]^+$ represents $\max\{\cdot, 0\}$; sign(x) represents the sign of x; $\mathcal{N}_c(\mu, \sigma^2)$ denotes the circularly symmetric complex Gaussian distribution with mean μ and variable σ^2.

B. System Model

In this paper, we consider a discrete memoryless MIMO TWRC in which users A and B exchange information via a relay, as illustrated in Fig. 1. User m is equipped with n_m antennas, $m \in \{A, B\}$, and the relay with n_R antennas. We assume that there is no direct link between the two users. The channel is assumed to be flat-fading and quasi-static, i.e., the channel coefficients remain unchanged during each round of information exchange. The channel matrix from user m to the relay is denoted by $\mathbf{H}_{mR} \in \mathbb{C}^{n_R \times n_m}$, and that from the relay to user m is denoted by $\mathbf{H}_{Rm} \in \mathbb{C}^{n_m \times n_R}, m \in \{A, B\}$. We further assume that the channel matrices are always of either full column rank or full row rank, whichever is smaller, and are globally known by both users as well as by the relay.

The system operates in a half-duplex mode. Two time-slots are employed for each round of information exchange. Following the convention in [16]-[18], we assume that the two time-slots have same duration. The extension of our results to the case of unequal duration is straightforward.

In the first time-slot (referred to as *uplink phase*), the two users transmit to the relay simultaneously and the relay remains silent. The transmit signal matrix at user m is denoted by $\mathbf{X}_m \in \mathbb{C}^{n_m \times T}$, $m \in \{A, B\}$, where T is the number of channel uses in one time-slot. Each column of $\mathbf{X}_m$ denotes the signal vector transmitted by the n_m antennas in one channel use. The average power at each user is constrained as $\frac{1}{T}E\left[\|\mathbf{X}_m\|_F^2\right] \leq P_m$, $m \in \{A, B\}$. The received signal at the relay is denoted by $\mathbf{Y}_R \in \mathbb{C}^{n_R \times T}$ with

$$\mathbf{Y}_R = \mathbf{H}_{AR}\mathbf{X}_A + \mathbf{H}_{BR}\mathbf{X}_B + \mathbf{Z}_R, \tag{1}$$

where $\mathbf{Z}_R \in \mathbb{C}^{n_R \times T}$ denotes the additive white Gaussian noise (AWGN) at the relay. We assume that the elements of $\mathbf{Z}_R$ are independent and identically drawn from $\mathcal{N}_c(0, N_0)$. Upon receiving $\mathbf{Y}_R$, the relay generates a signal matrix $\mathbf{X}_R \in \mathbb{C}^{n_R \times T}$.

In the second time-slot (referred to as *downlink phase*), $\mathbf{X}_R$ is broadcast to the two users. The average power at the relay is constrained as $\frac{1}{T}E\left[\|\mathbf{X}_R\|_F^2\right] \leq P_R$. The signal matrix received by user m is denoted by $\mathbf{Y}_m \in \mathbb{C}^{n_m \times T}, m \in \{A, B\}$, with

$$\mathbf{Y}_m = \mathbf{H}_{Rm}\mathbf{X}_R + \mathbf{Z}_m, m \in \{A, B\}, \tag{2}$$

where $\mathbf{Z}_m$ denotes the AWGN matrix at user m, with the elements independently drawn from $\mathcal{N}_c(0, N_0)$.

C. *Definition of Achievable Rates*

For the system model described above, denote the message of user m by $W_m \in \{1, 2, ..., 2^{2TR_m}\}$. The cardinality of W_m is given by 2^{2TR_m}, where the factor of $2T$ is because each round of information exchange consists of two length-T time-slots. At user A, the estimated message of user B, denoted by $\hat{W}_B$, is obtained from the received signal $\mathbf{Y}_A$ and the perfect knowledge of the self message W_A. The decoding operation at user B is similar. The error probability is defined as $P_e \triangleq \Pr\{\hat{W}_A \neq W_A \text{ or } \hat{W}_B \neq W_B\}$. We say that a rate-pair (R_A, R_B) is achievable if the error probability P_e vanishes as T tends to infinity. The achievable rate-region is defined as the closure of all possible achievable rate-pairs.

D. Capacity Upper Bound

Here we briefly describe a capacity upper bound of the MIMO TWRC. Let $\mathbf{Q}_m \triangleq \frac{1}{T}E\left[\mathbf{X}_m\mathbf{X}_m^\dagger\right], m \in \{A, B, R\}$, be the input covariance matrices. For given $\{\mathbf{Q}_A,\ \mathbf{Q}_B,\ \mathbf{Q}_R\}$ satisfying $\mathrm{tr}(\mathbf{Q}_m) \leq P_m, m \in \{A, B, R\}$, the achievable rate-pairs (R_A, R_B) of the MIMO TWRC is upper bounded as [16]

$$\begin{aligned} R_A &\leq \min\left\{R_A^{UL}\left(\mathbf{Q}_A\right), R_A^{DL}\left(\mathbf{Q}_R\right)\right\} && \text{(3a)} \\ R_B &\leq \min\left\{R_B^{UL}\left(\mathbf{Q}_B\right), R_B^{DL}\left(\mathbf{Q}_R\right)\right\} && \text{(3b)} \end{aligned}$$

where

$$\begin{aligned} R_m^{UL}\left(\mathbf{Q}_m\right) &= \frac{1}{2}\log\left|\mathbf{I}_{n_R} + \frac{1}{N_0}\mathbf{H}_{mR}\mathbf{Q}_m\mathbf{H}_{mR}^\dagger\right|, m \in \{A, B\} && \text{(4a)} \\ R_A^{DL}\left(\mathbf{Q}_R\right) &= \frac{1}{2}\log\left|\mathbf{I}_{n_B} + \frac{1}{N_0}\mathbf{H}_{RB}\mathbf{Q}_R\mathbf{H}_{RB}^\dagger\right|, && \text{(4b)} \\ R_B^{DL}\left(\mathbf{Q}_R\right) &= \frac{1}{2}\log\left|\mathbf{I}_{n_A} + \frac{1}{N_0}\mathbf{H}_{RA}\mathbf{Q}_R\mathbf{H}_{RA}^\dagger\right|. && \text{(4c)} \end{aligned}$$

Here, the superscripts “UL” and “DL” respectively represent uplink and downlink, and the factor of 1/2 is due to the two time-slots used for each round of information exchange.

A capacity-region outer bound is defined as the closure of the upper-bound rate-pairs in (3). This outer bound can be determined by optimizing $\mathbf{Q}_A$, $\mathbf{Q}_B$, and $\mathbf{Q}_R$, as detailed in [16] and [17]. The goal of this paper is to develop a communication strategy that can approach this outer bound.

III. RELAYING STRATEGIES FOR TWRCS WITH SINGLE-ANTENNA USERS

In this section, we study efficient communications over TWRCs with single-antenna users and a multi-antenna relay, i.e., $n_A = n_B = 1$ and $n_R \geq 1$. The results developed in this section will be used in our studies on general MIMO TWRCs later.

A. Relaying Strategies: Complete Decoding versus PNC

For the case of single-antenna users, the channel model of the uplink phase in (1) can be simplified as

$$\mathbf{Y}_R = \mathbf{h}_{AR}\mathbf{x}_A^T + \mathbf{h}_{BR}\mathbf{x}_B^T + \mathbf{Z}_R \tag{5}$$

where $\mathbf{h}_{mR} \in \mathbb{C}^{n_R \times 1}$ is the reduced version of $\mathbf{H}_{mR}$, and $\mathbf{x}_m \in \mathbb{C}^{T \times 1}$ is the transmit signal vector of user m, with the ith entry of $\mathbf{x}_m$ being the signal transmitted at the ith time interval, $m \in \{A, B\}$. Upon receiving $\mathbf{Y}_R$, the relay generates a network-coded message following the spirit of network coding. This network-coded message will be forwarded to the two users in the downlink phase.

The relay operation is detailed as follows. In the uplink phase, the signal direction of user m is given by $\mathbf{h}_{mR},\ m \in \{A, B\}$. On one hand, if $\mathbf{h}_{AR}$ and $\mathbf{h}_{BR}$ are orthogonal, both messages of the two users can be decoded free of interference from each other. The recovered messages of the two users are then network-coded and forwarded to the two users. We refer to this first strategy as the *complete-decoding (CD) strategy*. On the other hand, if $\mathbf{h}_{AR}$ and $\mathbf{h}_{BR}$ turn out to be parallel (i.e., in a same direction), then it is advantageous to compute a linear function of $\mathbf{x}_A$ and $\mathbf{x}_B$, referred to as a network-coded message, instead of completely decoding both $\mathbf{x}_A$ and $\mathbf{x}_B$. We refer to this second strategy as the *PNC strategy*.

In general, the following strategy can be adopted: if $\mathbf{h}_{AR}$ and $\mathbf{h}_{BR}$ tend to be orthogonal, the complete-decoding strategy is applied; if $\mathbf{h}_{AR}$ and $\mathbf{h}_{BR}$ tend to be parallel, the PNC strategy is applied. The selection between these two strategies is based on their achievable rates, as described below.

1) The Complete-Decoding Strategy: For complete-decoding, the uplink channel in (5) becomes a multiple-access (MAC) channel. Let $R_m^{CD}, m \in \{A, B\}$, be the rate of user m for the complete-decoding strategy. Then, the uplink rate-region of the complete-decoding strategy, denoted by $\mathcal{R}^{CD}$, is given by

$$R_A^{CD} + R_B^{CD} \leq \frac{1}{2}\log\left|\mathbf{I}_{n_R} + \sum_{m\in\{A,B\}} \frac{P_m}{N_0}\mathbf{h}_{mR}\mathbf{h}_{mR}^\dagger\right| \tag{6a}$$

$$R_m^{CD} \leq \frac{1}{2}\log\left(1 + \frac{P_m}{N_0}\mathbf{h}_{mR}^\dagger\mathbf{h}_{mR}\right), m \in \{A, B\}\,. \tag{6b}$$

which follows from the well-known MAC capacity region [24].

2) The PNC Strategy: For the PNC strategy in [5][6], it is required that the two user-signals lie in a same spatial direction. This is not guaranteed here due to the availability of multiple antennas at the relay.

To facilitate PNC, we next propose a projection-based method as follows. The signals from the two users are first projected to a common direction, denoted by a unit vector $\mathbf{p} \in \mathbb{C}^{n_R \times 1}$. The choice of $\mathbf{p}$ will be discussed in the next subsection. This projection operation creates an aligned scalar channel given by

$$\mathbf{p}^{\dagger}\mathbf{Y}_R = \mathbf{p}^{\dagger}\mathbf{h}_{AR}\mathbf{x}_A^T + \mathbf{p}^{\dagger}\mathbf{h}_{BR}\mathbf{x}_B^T + \mathbf{p}^{\dagger}\mathbf{Z}_R \tag{7}$$

with the effective channel coefficients given by $\mathbf{p}^{\dagger}\mathbf{h}_{AR}$ and $\mathbf{p}^{\dagger}\mathbf{h}_{BR}$.

From [16], if the sum of the two users' codewords, i.e., $\mathbf{p}^{\dagger}\mathbf{h}_{AR}\mathbf{x}_A^T + \mathbf{p}^{\dagger}\mathbf{h}_{BR}\mathbf{x}_B^T$, is required to be decoded, an achievable rate-pair (R_A^{PNC}, R_B^{PNC}) of the uplink phase is given by

$$R_m^{PNC} = \frac{1}{2}\left[\log\left(\frac{Q_m \left|\mathbf{p}^{\dagger}\mathbf{h}_{mR}\right|^2}{N_0}\right)\right]^+, m \in \{A, B\}, \tag{8}$$

where $Q_m = \frac{1}{T}E[\mathbf{x}_m^{\dagger}\mathbf{x}_m]$ represents the transmission power of user m. If $\mathbf{p}^{\dagger}\mathbf{h}_{AR}\mathbf{x}_A^T + \mathbf{p}^{\dagger}\mathbf{h}_{BR}\mathbf{x}_B^T$ is not necessarily decoded, the above rate-pair can be further improved by using the lattice-modulo operation and minimum mean-square error (MMSE) scaling [5][22], with the achievable rate-pair given by

$$R_m^{PNC} = \frac{1}{2}\left[\log\left(\frac{Q_m \left|\mathbf{p}^{\dagger}\mathbf{h}_{mR}\right|^2}{Q_A \left|\mathbf{p}^{\dagger}\mathbf{h}_{AR}\right|^2 + Q_B \left|\mathbf{p}^{\dagger}\mathbf{h}_{BR}\right|^2} + \frac{Q_m \left|\mathbf{p}^{\dagger}\mathbf{h}_{mR}\right|^2}{N_0}\right)\right]^+, m \in \{A, B\}. \tag{9}$$

Notice that (8) and (9) become identical and both approaches the uplink channel capacity at high SNR.

The uplink rate-region of the PNC scheme is given by

$$\mathcal{R}^{PNC} \triangleq \left\{(R_A, R_B) | R_m \leq R_m^{PNC}, Q_m \leq P_m, m \in \{A, B\}, \mathbf{p}^{\dagger}\mathbf{p} = \mathbf{1}\right\}. \tag{10}$$

The boundary of $\mathcal{R}^{PNC}$ can be found by optimizing Q_A, Q_B, and $\mathbf{p}$, as detailed in the next subsection.

B. Optimization of Projection Direction

Here we focus on the rate-pair given in (8).[1] As achievable rate-regions are convex, the boundary points of $\mathcal{R}^{PNC}$ can be determined by solving the weighted sum-rate maximization problem:

$$\text{maximize} \quad w_A R_A^{PNC} + w_B R_B^{PNC} \tag{11a}$$

$$\text{subject to} \quad ||\mathbf{p}|| = 1, Q_m \leq P_m, m \in \{A, B\} \tag{11b}$$

where w_A and w_B are arbitrary nonnegative weighting coefficients. By inspecting (8), the maximum of (11) is achieved at $Q_m = P_m, m \in \{A, B\}$. Thus, we only need to optimize $\mathbf{p}$.

---

[1] The treatment for the rate-pair in (9) is similar, and thus omitted.

Suppose that $R_A^{PNC} = 0$ (or $R_B^{PNC} = 0$). Then, from (8), the optimal $\mathbf{p}$ is trivially taken as $\frac{\mathbf{h}_{BR}}{\|\mathbf{h}_{BR}\|}$ (or $\frac{\mathbf{h}_{AR}}{\|\mathbf{h}_{AR}\|}$). Thus, we focus on the case of $R_m^{PNC} > 0, m \in \{A, B\}$. In this case, this weighted sum-rate maximization problem is equivalent to maximizing

$$\max_{||\mathbf{p}||=1} w_A \log\left(\left|\mathbf{p}^\dagger \mathbf{h}_{AR}\right|^2\right) + w_B \log\left(\left|\mathbf{p}^\dagger \mathbf{h}_{BR}\right|^2\right) \tag{12}$$

or equivalently

$$\max_{||\widetilde{\mathbf{p}}||=1} \left|\widetilde{\mathbf{h}}_{AR}^T \widetilde{\mathbf{p}}\right|^{2w_A} \left|\widetilde{\mathbf{h}}_{BR}^T \widetilde{\mathbf{p}}\right|^{2w_B}$$

where $\widetilde{\mathbf{p}} = [\mathrm{Re}[\mathbf{p}^T], \mathrm{Im}[\mathbf{p}^T]]^T$ and $\widetilde{\mathbf{h}}_{mR} = [\mathrm{Re}[\mathbf{h}_{mR}^T], \mathrm{Im}[\mathbf{h}_{mR}^T]]^T$, $m \in \{A, B\}$. By setting the derivative of the Lagrangian with respect to $\mathbf{p}$ to zero, the optimal $\mathbf{p}$ satisfies

$$\alpha \widetilde{\mathbf{p}} = \frac{w_A \widetilde{\mathbf{h}}_{AR}}{\widetilde{\mathbf{p}}^T \widetilde{\mathbf{h}}_{AR}} + \frac{w_B \widetilde{\mathbf{h}}_{BR}}{\widetilde{\mathbf{p}}^T \widetilde{\mathbf{h}}_{BR}},$$

where α is a scaling factor. Then, with some straightforward algebra, we obtain the optimal projection direction given by

$$\widetilde{\mathbf{p}}^{opt} = \gamma \left(\frac{\widetilde{\mathbf{h}}_{AR}}{\left\|\widetilde{\mathbf{h}}_{AR}\right\|} + \beta \frac{\widetilde{\mathbf{h}}_{BR}}{\left\|\widetilde{\mathbf{h}}_{BR}\right\|} \right), \tag{13}$$

where

$$\beta = \frac{\mathrm{sign}(\widetilde{\mathbf{h}}_{AR}^T \widetilde{\mathbf{h}}_{BR})}{2} \left(\sqrt{ \left(\frac{\widetilde{\mathbf{h}}_{AR}^T \widetilde{\mathbf{h}}_{BR} \left(1 - \frac{w_B}{w_A}\right)}{\left\|\widetilde{\mathbf{h}}_{AR}\right\| \left\|\widetilde{\mathbf{h}}_{BR}\right\|} \right)^2 + 4 \frac{w_B}{w_A} } - \frac{\left|\widetilde{\mathbf{h}}_{AR}^T \widetilde{\mathbf{h}}_{BR}\right| \left(1 - \frac{w_B}{w_A}\right)}{\left\|\widetilde{\mathbf{h}}_{AR}\right\| \left\|\widetilde{\mathbf{h}}_{BR}\right\|} \right) \tag{14}$$

and γ is a scaling factor to ensure $||\widetilde{\mathbf{p}}^{opt}|| = 1$. Particularly, for the sum-rate case, i.e., $w_A = w_B = 1$, the optimal projection direction $\widetilde{\mathbf{p}}$ is just the angular bisector of $\widetilde{\mathbf{h}}_{AR}$ and $\widetilde{\mathbf{h}}_{BR}$ if $\widetilde{\mathbf{h}}_{AR}^T \widetilde{\mathbf{h}}_{BR} > 0$, or the angular bisector of $\widetilde{\mathbf{h}}_{AR}$ and $-\widetilde{\mathbf{h}}_{BR}$ if $\widetilde{\mathbf{h}}_{AR}^T \widetilde{\mathbf{h}}_{BR} < 0$. By varying w_A and w_B, $\mathcal{R}^{PNC}$ can be determined.

C. The Overall Scheme

For the uplink phase, the achievable rate-regions $\mathcal{R}^{CD}$ and $\mathcal{R}^{PNC}$, for certain channel realizations of $\mathbf{h}_{AR}$ and $\mathbf{h}_{BR}$, are depicted in Fig. 2. The overall uplink rate-region, denoted by $\mathcal{R}^{UL}$, is given by the convex hull of $\mathcal{R}^{CD}$ and $\mathcal{R}^{PNC}$. In the overall scheme, the relay will select between the complete-decoding and PNC strategies for a larger achievable rate-region, according to (6) and (10).

For the downlink phase, the achievable rate-region is determined as follows. For the complete-decoding strategy, the relay jointly re-encode the decoded messages $\mathbf{x}_A$ and $\mathbf{x}_B$, and forward the resulting codeword to the two users in the downlink. For the PNC strategy, the relay forward the lattice-modulo of $\mathbf{p}^\dagger\mathbf{h}_{AR}\mathbf{x}_A^T + \mathbf{p}^\dagger\mathbf{h}_{BR}\mathbf{x}_B^T$, referred to as a network-coded message, to the two users. Then each user recovers the message of the other user with the help of the perfect knowledge of self message. From [16]-[18], the downlink rate-region $\mathcal{R}^{DL}$ for the two strategies are the same and given by

$$\mathcal{R}^{DL} \triangleq \left\{(R_A, R_B) | R_A \leq R_A^{DL}, R_B \leq R_B^{DL}\right\} \tag{15}$$

with

$$R_A^{DL} = \frac{1}{2}\log\left(1 + \frac{P_R}{N_0}\mathbf{h}_{RB}^\dagger\mathbf{h}_{RB}\right) \text{ and } R_B^{DL} = \frac{1}{2}\log\left(1 + \frac{P_R}{N_0}\mathbf{h}_{RA}^\dagger\mathbf{h}_{RA}\right). \tag{16}$$

Finally, an achievable rate-region of the overall scheme is the intersection of the uplink rate-region $\mathcal{R}^{UL}$ and the downlink rate-region $\mathcal{R}^{DL}$.

IV. SPACE-DIVISION APPROACH FOR MIMO TWRCS

In the preceding section, we have studied the design of relaying strategies for TWRCs with single-antenna users. We have shown how to exploit the benefits of the complete-decoding and PNC strategies. In this section, we proceed to study the general case of $n_A \geq 1$, $n_B \geq 1$. We propose a new space-division based network-coding scheme, as a generalization for the case of single-antenna users.

A. Motivations

What motivates the proposed space-division approach is the following property of $\mathbf{H}_{AR}$ and $\mathbf{H}_{BR}$. Denote by $\mathcal{C}(\mathbf{H}_{AR})$ and $\mathcal{C}(\mathbf{H}_{BR})$ the columnspaces of the uplink channel matrices $\mathbf{H}_{AR}$ and $\mathbf{H}_{BR}$, respectively. In general, we can partition the columnspace $\mathcal{C}(\mathbf{H}_{AR}) \in \mathbb{C}^{n_R}$ as the direct sum[2] of three orthogonal subspaces: a subspace $\mathcal{S}_{A\|B}$ that is parallel to $\mathcal{C}(\mathbf{H}_{BR})$, i.e., any vector in $\mathcal{S}_{A\|B}$ belongs to $\mathcal{C}(\mathbf{H}_{BR})$; a subspace $\mathcal{S}_{A\nparallel B}$ that is neither parallel nor orthogonal to $\mathcal{C}(\mathbf{H}_{BR})$; and a subspace $\mathcal{S}_{A\perp B}$ that is orthogonal to $\mathcal{C}(\mathbf{H}_{BR})$. Similarly, $\mathcal{C}(\mathbf{H}_{BR})$ is the direct sum of three orthogonal subspaces $\mathcal{S}_{B||A}, \mathcal{S}_{B\nparallel A}$, and $\mathcal{S}_{B\perp A}$. Note that $\mathcal{S}_{A\|B} = \mathcal{S}_{B||A}$ since both represent the *common space* of $\mathcal{C}(\mathbf{H}_{AR})$ and $\mathcal{C}(\mathbf{H}_{BR})$.

---

[2] Let $\mathcal{S}$ be a vector space, and let $\mathcal{S}_1, \mathcal{S}_2, ..., \mathcal{S}_n$ be subspaces of $\mathcal{S}$. $\mathcal{S}$ is defined to be a direct sum of $\mathcal{S}_1, \mathcal{S}_2, ..., \mathcal{S}_n$ when $\mathcal{S}_1, \mathcal{S}_2, ..., \mathcal{S}_n$ are mutually orthogonal and for every vector $\mathbf{x}$ in $\mathcal{S}$, there is $\mathbf{x}_i$ in $\mathcal{S}_i, i = 1, 2, ..., n$, such that $\mathbf{x} = \sum_{i=1}^{n}\mathbf{x}_i$.

In $\mathcal{S}_{A\|B}$, the signal directions of the two users can be efficiently aligned to a same set of directions, providing a platform to carry out PNC, as in [16]-[18]. On the other hand, in $\mathcal{S}_{A\perp B}$ or $\mathcal{S}_{B\perp A}$, the two users do not interfere with each other, hence the complete-decoding strategy can be employed. The above treatments are similar to those for the case of single-antenna users, as discussed in the preceding section. What remains is the treatment for the signals in $\mathcal{S}_{A\nparallel B}$ and $\mathcal{S}_{B\nparallel A}$ that are neither parallel nor orthogonal. Heuristically, some channel directions in $\mathcal{S}_{A\nparallel B}$ and $\mathcal{S}_{B\nparallel A}$ may be nearly parallel to each other. For these channel directions, the PNC strategy is preferable for the related spatial streams. On the other hand, some channel directions in $\mathcal{S}_{A\nparallel B}$ and $\mathcal{S}_{B\nparallel A}$ may be nearly orthogonal to each other. Then, the complete-decoding strategy is preferable. The main challenge lies in how to identify those nearly parallel/orthogonal channel directions. To this end, we next propose a new joint channel decomposition.

B. *Joint Channel Decomposition*

Let the compact singular value decomposition (SVD) of $\mathbf{H}_{mR}$ be

$$\mathbf{H}_{mR} = \mathbf{U}_m \boldsymbol{\Delta}_m \mathbf{V}_m^{\dagger},\ m \in \{A, B\} \tag{17}$$

where $\mathbf{U}_m$ is an n_R-by-n_m orthonormal matrix with $\mathbf{U}_m^{\dagger}\mathbf{U}_m = \mathbf{I}_{n_m}$.

Denote by λ_i the ith eigenvalue of the matrix $\mathbf{U}_A\mathbf{U}_A^{\dagger} + \mathbf{U}_B\mathbf{U}_B^{\dagger}$, and by $\mathbf{u}_i$ the corresponding eigenvector. Without loss of generality, we arrange $\{\lambda_i\}$ in the descending order. As the eigenvalues of $\mathbf{U}_m\mathbf{U}_m^{\dagger}$ are either 1 or 0, the eigenvalues $\{\lambda_i\}$ are valued between 0 and 2. Note that $\lambda_i = 2$ implies that $\mathbf{U}_A\mathbf{U}_A^{\dagger}\mathbf{u}_i = \mathbf{u}_i$ and $\mathbf{U}_B\mathbf{U}_B^{\dagger}\mathbf{u}_i = \mathbf{u}_i$. This means that $\mathbf{u}_i$ is in the common space $\mathcal{S}_{A\|B}$ of $\mathbf{H}_{AR}$ and $\mathbf{H}_{BR}$. Also note that $\lambda_i = 1$ implies $\{\mathbf{U}_A\mathbf{U}_A^{\dagger}\mathbf{u}_i = \mathbf{u}_i$, $\mathbf{U}_B\mathbf{U}_B^{\dagger}\mathbf{u}_i = \mathbf{0}\}$ or $\{\mathbf{U}_A\mathbf{U}_A^{\dagger}\mathbf{u}_i = \mathbf{0}$, $\mathbf{U}_B\mathbf{U}_B^{\dagger}\mathbf{u}_i = \mathbf{u}_i\}$ (cf., Theorem 4.3.4 in [29]). That is, $\mathbf{u}_i$ is in $\mathcal{S}_{A\perp B}$ (or $\mathcal{S}_{B\perp A}$) which is orthogonal to the space spanned by $\mathbf{H}_{BR}$ (or $\mathbf{H}_{AR}$). In addition, the number of eigenvalues between 1 and 2 is the same as that between 0 and 1, as we will see later.

Let k be the number of eigenvalues of $\mathbf{U}_A\mathbf{U}_A^{\dagger} + \mathbf{U}_B\mathbf{U}_B^{\dagger}$ equal to 2; l be the number of eigenvalues between 1 and 2; d_A be the number of eigenvalues equal to 1 with $\{\mathbf{U}_A\mathbf{U}_A^{\dagger}\mathbf{u}_i = \mathbf{u}_i$, $\mathbf{U}_B\mathbf{U}_B^{\dagger}\mathbf{u}_i = \mathbf{0}\}$; d_B be the number of eigenvalues equal to 1 with $\{\mathbf{U}_A\mathbf{U}_A^{\dagger}\mathbf{u}_i = \mathbf{0}$, $\mathbf{U}_B\mathbf{U}_B^{\dagger}\mathbf{u}_i = \mathbf{u}_i\}$. Also let $\mathbf{U} \in \mathbb{C}^{n_R\times(n_A+n_B-k)}$ be a matrix with the columns consisting of the eigenvectors corresponding to the $n_A + n_B - k$ largest eigenvalues of

$\mathbf{U}_A\mathbf{U}_A^\dagger + \mathbf{U}_B\mathbf{U}_B^\dagger$ (as specified in (70)). Due to the orthogonality of the eigenvectors, $\mathbf{U}$ is orthonormal, i.e., $\mathbf{U}^\dagger\mathbf{U} = \mathbf{I}_{n_A+n_B-k}$.

We are now ready to present the joint channel decomposition, with the proof given in Appendix A.

Theorem 1: The channel matrices $\mathbf{H}_{AR}$ and $\mathbf{H}_{BR}$ can be jointly decomposed as

$$\mathbf{H}_{mR} = \mathbf{U}\mathbf{D}_m\mathbf{G}_m, \ m \in \{A, B\} \tag{18}$$

where $\mathbf{G}_m \in \mathbb{C}^{n_m \times n_m}$ is a square matrix, and $\mathbf{D}_m \in \mathbb{C}^{(n_A+n_B-k)\times n_m}, m \in \{A, B\}$, are orthonormal matrices with a block-diagonal structure given by

$$\mathbf{D}_A = \begin{bmatrix} \mathbf{I}_k & \mathbf{0} & \mathbf{0} \\ \mathbf{0} & \mathbf{E}_A & \mathbf{0} \\ \mathbf{0} & \mathbf{0} & \mathbf{I}_{d_A} \\ \mathbf{0} & \mathbf{0} & \mathbf{0} \end{bmatrix} \text{ and } \mathbf{D}_B = \begin{bmatrix} \mathbf{I}_k & \mathbf{0} & \mathbf{0} \\ \mathbf{0} & \mathbf{E}_B & \mathbf{0} \\ \mathbf{0} & \mathbf{0} & \mathbf{0} \\ \mathbf{0} & \mathbf{0} & \mathbf{I}_{d_B} \end{bmatrix} \tag{19a}$$

with

$$\mathbf{E}_m = \begin{bmatrix} \mathbf{e}_{m;k+1} & \mathbf{0} & \cdots & \mathbf{0} \\ \mathbf{0} & \mathbf{e}_{m;k+2} & \ddots & \vdots \\ \vdots & \ddots & \ddots & \mathbf{0} \\ \mathbf{0} & \cdots & \mathbf{0} & \mathbf{e}_{m;k+l} \end{bmatrix} \in \mathbb{C}^{2l\times l}, \tag{19b}$$

$$\mathbf{e}_{A;i} = \begin{bmatrix} \sqrt{\frac{\lambda_i}{2}} \\ \sqrt{\frac{2-\lambda_i}{2}} \end{bmatrix} \text{ and } \mathbf{e}_{B;i} = \begin{bmatrix} \sqrt{\frac{\lambda_i}{2}} \\ -\sqrt{\frac{2-\lambda_i}{2}} \end{bmatrix}. \tag{19c}$$

Remark 1: From (18), we see that $\mathcal{C}(\mathbf{U})$ is the overall columnspace of the two channel matrices, i.e., $\mathcal{C}(\mathbf{U}) = \mathcal{C}([\mathbf{H}_{AR}\ \mathbf{H}_{BR}])$. Moreover, $\mathbf{U}\mathbf{D}_m$ specifies the columnspace of $\mathbf{H}_m$, i.e., $\mathcal{C}(\mathbf{U}\mathbf{D}_m) = \mathcal{C}(\mathbf{H}_m)$. Note that $\mathbf{U}\mathbf{D}_m$ is orthonormal, as $\mathbf{D}_m^\dagger\mathbf{U}^\dagger\mathbf{U}\mathbf{D}_m = \mathbf{I}_{n_m}$, $m \in \{A, B\}$. Therefore, the columns of $\mathbf{U}\mathbf{D}_m$ give an orthogonal basis of $\mathcal{C}(\mathbf{H}_{mR})$, with the coordinates of $\mathbf{H}_{mR}$ specified in $\mathbf{G}_m$.

Remark 2: The column structures of $\mathbf{U}\mathbf{D}_A$ and $\mathbf{U}\mathbf{D}_B$ are explained as follows. In the first place, we note that $\mathbf{U}\mathbf{D}_A$ and $\mathbf{U}\mathbf{D}_B$ share the same first k columns. Thus, the first k columns of $\mathbf{U}\mathbf{D}_A$ span $\mathcal{S}_{A\|B}$, i.e., the common space of $\mathcal{C}(\mathbf{H}_{AR})$ and $\mathcal{C}(\mathbf{H}_{BR})$. Second, from (19a), the last d_A columns of $\mathbf{U}\mathbf{D}_A$ (obtained from multiplying $\mathbf{U}$ with the third block column of $\mathbf{D}_A$) are orthogonal to $\mathbf{U}\mathbf{D}_B$. Hence, these columns of $\mathbf{U}\mathbf{D}_A$ span the subspace $\mathcal{S}_{A\perp B}$, i.e., the subspace orthogonal to $\mathcal{C}(\mathbf{H}_{BR})$. Third, the remaining l columns of $\mathbf{U}\mathbf{D}_A$

span the subspace $\mathcal{S}_{A\nparallel B}$, by noting the facts that $\mathcal{C}(\mathbf{H}_{AR}) = \mathcal{C}(\mathbf{UD}_A)$ and that $\mathcal{C}(\mathbf{H}_{AR})$ is the direct-sum of three orthogonal subspaces $\mathcal{S}_{A\|B}$, $\mathcal{S}_{A\nparallel B}$, and $\mathcal{S}_{A\perp B}$. Similarly, the first k columns of $\mathbf{UD}_B$ span $\mathcal{S}_{A\|B}$, the next l columns span $\mathcal{S}_{B\nparallel A}$, and the last d_B columns span $\mathcal{S}_{B\perp A}$. Recall that $\mathcal{C}(\mathbf{H}_{AR})$ is the direct sum of $\mathcal{S}_{A\|B}$, $\mathcal{S}_{A\nparallel B}$, and $\mathcal{S}_{A\perp B}$, and that $\mathcal{C}(\mathbf{H}_{BR})$ is the direct sum of $\mathcal{S}_{B\|A}$, $\mathcal{S}_{B\nparallel A}$, and $\mathcal{S}_{B\perp A}$. Thus, the dimensions of these subspaces have the following relationship:

$$k + l + p_m = n_m, m \in \{A, B\}\,. \tag{20}$$

We summarize the geometrical meanings of the aforementioned subspaces and their dimensions as follows.

Subspace	Dimension	Property
$\mathcal{S}_{A\|B}$	k	common space of $\mathcal{C}(\mathbf{H}_{AR})$ and $\mathcal{C}(\mathbf{H}_{BR})$
$\mathcal{S}_{A\nparallel B}$	l	not parallel/orthogonal to $\mathcal{C}(\mathbf{H}_{BR})$
$\mathcal{S}_{B\nparallel A}$	l	not parallel/orthogonal to $\mathcal{C}(\mathbf{H}_{AR})$
$\mathcal{S}_{A\perp B}$	d_A	orthogonal to $\mathcal{C}(\mathbf{H}_{BR})$
$\mathcal{S}_{B\perp A}$	d_B	orthogonal to $\mathcal{C}(\mathbf{H}_{AR})$

Let $\mathbf{v}_{m;i}$ be the ith column of $\mathbf{UD}_m$, $m \in \{A, B\}$. We refer to $\mathbf{v}_{A;i}$ and $\mathbf{v}_{B;i}$ as the ith *channel direction pair*. Here, $\mathbf{v}_{A;i}^\dagger \mathbf{v}_{B;i} = 1$ means that $\mathbf{v}_{A;i}$ and $\mathbf{v}_{B;i}$ are parallel, and $\mathbf{v}_{A;i}^\dagger \mathbf{v}_{B;i} = 0$ means that they are orthogonal. Thus, $\mathbf{v}_{A;i}^\dagger \mathbf{v}_{B;i}$ can be regarded as a measure of the *degree of orthogonality* of $\mathbf{v}_{A;i}$ and $\mathbf{v}_{B;i}$. In the following corollary, the degree of orthogonality of each channel direction pair ($\mathbf{v}_{A;i}$, $\mathbf{v}_{B;i}$) is determined by the magnitude of λ_i, i.e., the ith eigenvalue of $\mathbf{U}_A\mathbf{U}_A^\dagger + \mathbf{U}_B\mathbf{U}_B^\dagger$.

Corollary 1: For $i = 1, ..., k + l$, the degree of orthogonality of the ith channel direction pair ($\mathbf{v}_{A,i}$, $\mathbf{v}_{B,i}$) is given by $\mathbf{v}_{A,i}^\dagger \mathbf{v}_{B,i} = \lambda_i - 1$.

Proof: For $i = 1, ..., k$, we see from (19a) that $\lambda_i = 2$ and $\mathbf{v}_{A;i} = \mathbf{v}_{B;i}$, and so $\mathbf{v}_{A;i}^\dagger \mathbf{v}_{B;i} = \lambda_i - 1$. For $i = k + 1, ..., k + l$, from (19a) and (19b), the ith column of $\mathbf{UD}_m$ is given by

$$\mathbf{v}_{m;i} = \begin{bmatrix} \widetilde{\mathbf{u}}_{2i-k-1} & \widetilde{\mathbf{u}}_{2i-k} \end{bmatrix} \mathbf{e}_{m;i}, \;\; m \in \{A, B\}\,, \tag{21}$$

where $\widetilde{\mathbf{u}}_i$ represents the ith column of $\mathbf{U}$. Then, we obtain $\mathbf{v}_{A;k+i}^\dagger \mathbf{v}_{B;k+i} = \mathbf{e}_{A;k+i}^\dagger \mathbf{e}_{B;k+i} = \lambda_i - 1$, where the first step utilizes the fact that $\mathbf{U}$ is orthonormal, and the second step follows from (19c). ■

Corollary 2: For $i = k+l+1, ..., n_A$, $\mathbf{v}_{A;i}$ is an eigenvector of $\mathbf{U}_A\mathbf{U}_A^\dagger + \mathbf{U}_B\mathbf{U}_B^\dagger$ corresponding to $\lambda_i = 1$, and is orthogonal to $\mathcal{C}(\mathbf{H}_{BR})$; for $i = k+l+1, ..., n_B$, $\mathbf{v}_{B;i}$ is an eigenvector corresponding to $\lambda_i = 1$, and is orthogonal to $\mathcal{C}(\mathbf{H}_{AR})$.

Remark 3: The above corollaries show that the eigenvalue λ_i is an indicator of the degree of orthogonality of the ith direction pair. In particular, $\lambda_i \approx 2$ means that the two channel directions are close to parallel; and $\lambda_i \approx 1$ means that the two channel directions are close to orthogonal.

Remark 4: Before leaving this subsection, we emphasize that the joint channel decomposition in Theorem 1 is general for any sizes of $\mathbf{H}_{AR}$ and $\mathbf{H}_{BR}$. Particularly, if $n_m \geq n_R, m \in \{A, B\}$, then $k = n_R$ and $l = 0$, implying that all the eigenvalues $\{\lambda_i\}$ are valued at 2. In this case, $\mathbf{H}_{AR}$ and $\mathbf{H}_{BR}$ span the same columnspace. Channel alignment techniques have been proposed in [16]-[18] for efficient implementation of PNC. In what follows, we are mainly interested in the case of $n_A, n_B < n_R$, i.e., there exist $\{\lambda_i\}$ valued between, but not including, 1 and 2.

C. Space-Division Approach for MIMO Two-Way Relaying

Based on the joint channel decomposition in Theorem 1, we now propose a new space-division approach for MIMO two-way relaying. The main idea is to divide the overall signal space $\mathcal{C}([\mathbf{H}_{AR}\ \mathbf{H}_{BR}]) = \mathcal{C}(\mathbf{U})$ into two orthogonal subspaces: 1) $\mathcal{S}^{PNC}$, in which the channel direction pairs $(\mathbf{v}_{A;i}, \mathbf{v}_{B;i})$ are parallel or close to parallel, for carrying out PNC; 2) $\mathcal{S}^{CD}$ for carrying out the complete-decoding strategy. Let l' be an arbitrary integer between 0 and l. Recall that the channel direction pairs are ordered by the degree of orthogonality as in Corollary 1. Therefore, the first $k + l'$ direction pairs have lower degree of orthogonality compared to the remaining pairs. Thus, we allocate the first $k + l'$ direction pairs to form a basis of $\mathcal{S}^{PNC}$. The remaining channel directions give a basis of $\mathcal{S}^{CD}$. In this section, we assume that l' is given. The details on the optimization of l' will be discussed later in Sections V and VI.

1) Space-Division Operation: Let the RQ decomposition of $\mathbf{G}_m$ be

$$\mathbf{G}_m = \mathbf{R}_m\mathbf{T}_m^\dagger,\ m \in \{A, B\} \tag{22}$$

where $\mathbf{R}_m \in \mathbb{C}^{n_m \times n_m}$ is an upper-triangular matrix given by

$$\mathbf{R}_m = \begin{bmatrix} r_{m;1,1} & r_{m;1,2} & \cdots & r_{m;1,n_m} \\ 0 & r_{m;2,2} & \cdots & r_{m;2,n_m} \\ \vdots & \vdots & \ddots & \vdots \\ 0 & \cdots & 0 & r_{m;n_m,n_m} \end{bmatrix}, \tag{23}$$

and $\mathbf{T}_m \in \mathbb{C}^{n_m \times n_m}$ is unitary. Together with (18), the channel matrices can be jointly decomposed as

$$\mathbf{H}_m = \mathbf{U}\mathbf{D}_m\mathbf{R}_m\mathbf{T}_m^{\dagger}, \ m \in \{A, B\}. \tag{24}$$

Then, the received signal at the relay, after left-multiplying $\mathbf{U}^{\dagger}$, can be represented as

$$\mathbf{Y}'_R = \mathbf{U}^{\dagger}\mathbf{Y}_R = \mathbf{D}_A\mathbf{R}_A\mathbf{X}'_A + \mathbf{D}_B\mathbf{R}_B\mathbf{X}'_B + \mathbf{Z}'_R, \tag{25}$$

where $\mathbf{X}'_m = \mathbf{T}_m^{\dagger}\mathbf{X}_m, m \in \{A, B\}$, and $\mathbf{Z}'_R = \mathbf{U}^{\dagger}\mathbf{Z}_R$ with i.i.d. elements $\sim \mathcal{N}_c(0, N_0)$.

We partition $\mathbf{R}_m$ and $\mathbf{D}_m$ as

$$\mathbf{R}_m = \begin{bmatrix} \mathbf{R}_{m;1,1} & \mathbf{R}_{m;1,2} \\ \mathbf{0} & \mathbf{R}_{m;2,2} \end{bmatrix} \text{ and } \mathbf{D}_m = \begin{bmatrix} \mathbf{D}_{m;1,1} & \mathbf{0} \\ \mathbf{0} & \mathbf{D}_{m;2,2} \end{bmatrix}, m \in \{A, B\} \tag{26}$$

where $\mathbf{R}_{m;1,1} \in \mathbb{C}^{(k+l') \times (k+l')}$ and $\mathbf{R}_{m;2,2} \in \mathbb{C}^{(l-l'+p_m) \times (l-l'+p_m)}$, $m \in \{A, B\}$, are upper triangular matrices, and $\mathbf{D}_{m;1,1} \in \mathbb{C}^{(k+2l') \times (k+l)}$ and $\mathbf{D}_{m;2,2} \in \mathbb{C}^{(n_R-k-2l') \times (l-l'+p_m)}, m \in \{A, B\}$, are block-diagonal matrices. Then, (25) can be written as

$$\begin{bmatrix} \mathbf{Y}_R^{PNC} \\ \mathbf{Y}_R^{CD} \end{bmatrix} = \sum_{m \in \{A,B\}} \begin{bmatrix} \mathbf{D}_{m;1,1}\mathbf{R}_{m;1,1} & \mathbf{D}_{m;1,1}\mathbf{R}_{m;1,2} \\ \mathbf{0} & \mathbf{D}_{m;2,2}\mathbf{R}_{m;2,2} \end{bmatrix} \begin{bmatrix} \mathbf{X}_m^{PNC} \\ \mathbf{X}_m^{CD} \end{bmatrix} + \begin{bmatrix} \mathbf{Z}_R^{PNC} \\ \mathbf{Z}_R^{CD} \end{bmatrix}, \tag{27}$$

where $\mathbf{Y}'_R$, $\mathbf{X}'_m$, and $\mathbf{Z}'_R$ are correspondingly partitioned as

$$\mathbf{Y}'_R = \begin{bmatrix} \mathbf{Y}_R^{PNC} \\ \mathbf{Y}_R^{CD} \end{bmatrix}, \mathbf{X}'_m = \begin{bmatrix} \mathbf{X}_m^{PNC} \\ \mathbf{X}_m^{CD} \end{bmatrix}, \text{ and } \mathbf{Z}'_R = \begin{bmatrix} \mathbf{Z}_R^{PNC} \\ \mathbf{Z}_R^{CD} \end{bmatrix}. \tag{28}$$

Here, the superscript “PNC” (or “CD”) represents the PNC (or complete-decoding) strategy.

Based on the signal model in (27), the proposed space-division based relaying strategy is described as follows. At user m, two groups of spatial streams are generated: one group, referred to as the *complete-decoding spatial streams*, form the codeword matrix $\mathbf{X}_m^{CD}$; and the other group, referred to as the *PNC spatial streams*, form the codeword matrix $\mathbf{X}_m^{PNC}$, $m \in \{A, B\}$.

2) Complete-Decoding Spatial Streams: Due to the block triangular structure of the channel matrices in (27), the relay can completely decode the spatial streams $\mathbf{X}_A^{CD}$ and $\mathbf{X}_B^{CD}$ free of interference from the PNC spatial streams. Specifically, the relay completely decodes both $\mathbf{X}_A^{CD}$ and $\mathbf{X}_B^{CD}$ based on

$$\mathbf{Y}_R^{CD} = \sum_{m\in\{A,B\}} \mathbf{D}_{m;2,2}\mathbf{R}_{m;2,2}\mathbf{X}_m^{CD} + \mathbf{Z}_R^{CD}. \tag{29}$$

Then, $\mathbf{X}_A^{CD}$ and $\mathbf{X}_B^{CD}$ are canceled from the received signal in (27).

3) PNC Spatial Streams: After the cancelation of $\mathbf{X}_A^{CD}$ and $\mathbf{X}_B^{CD}$, the system model for the PNC spatial streams is given by

$$\mathbf{Y}_R^{PNC} = \sum_{m\in\{A,B\}} \mathbf{D}_{m;1,1}\mathbf{R}_{m;1,1}\mathbf{X}_m^{PNC} + \mathbf{Z}_R^{PNC}. \tag{30}$$

From (19a), the first k columns of $\mathbf{D}_{A;1,1}$ and $\mathbf{D}_{B;1,1}$ are identical; however, for $i = k+1, ..., k+l'$, the ith columns of $\mathbf{D}_{A;1,1}$ and $\mathbf{D}_{B;1,1}$ are not. Following Section III, we project each column pair of $\mathbf{D}_{A;1,1}$ and $\mathbf{D}_{B;1,1}$ onto a common direction, so as to facilitate PNC.

By inspection, the only difference between the ith columns of $\mathbf{D}_{A;1,1}$ and $\mathbf{D}_{B;1,1}$ is given by the 2-by-1 vectors $\mathbf{e}_{A;i}$ and $\mathbf{e}_{B;i}$, for $i = k+1, ..., k+l'$. Without loss of generality, denote by $\mathbf{p}_i$ a 2-by-1 unit vector representing the projection direction of $\mathbf{e}_{A;i}$ and $\mathbf{e}_{B;i}$. The choice of $\mathbf{p}_i$ is similar to that described in Section III and will be detailed in the next section.

Now the projection process can be described in a matrix form as follows. Define the projection matrix

$$\mathbf{P} = \begin{bmatrix} \mathbf{I}_k & \mathbf{0} & \cdots & \mathbf{0} \\ \mathbf{0} & \mathbf{p}_{k+1} & \ddots & \vdots \\ \vdots & \ddots & \ddots & \mathbf{0} \\ \mathbf{0} & \cdots & \mathbf{0} & \mathbf{p}_{k+l'} \end{bmatrix} \in \mathbb{C}^{(k+2l')\times(k+l')}. \tag{31}$$

After the projection, the resulting signal model is given by

$$\widetilde{\mathbf{Y}}_R^{PNC} = \mathbf{P}^T\mathbf{Y}_R^{PNC} = \sum_{m\in\{A,B\}} \widetilde{\mathbf{H}}_m^{PNC}\mathbf{X}_m^{PNC} + \widetilde{\mathbf{Z}}_R^{PNC} \tag{32}$$

where $\widetilde{\mathbf{H}}_m^{PNC} = \mathbf{P}^T\mathbf{D}_{m;1,1}\mathbf{R}_{m;1,1} = \tilde{\mathbf{D}}_{m;1,1}\mathbf{R}_{m;1,1} \in \mathbb{C}^{(k+l')\times(k+l')}$, with

$$\tilde{\mathbf{D}}_{m;1,1} = \text{diag}\left\{1, ..., 1, \mathbf{p}_{k+1}^T\mathbf{e}_{m;k+1}, ..., \mathbf{p}_{k+l'}^T\mathbf{e}_{m;k+l'}\right\}, m \in \{A, B\}, \tag{33}$$

and $\widetilde{\mathbf{Z}}_R^{PNC} = \mathbf{P}^T\mathbf{Z}_R^{PNC} \in \mathbb{C}^{(n_R-l')\times 1}$ with the entries being i.i.d. random variables $\sim \mathcal{N}_c(0, N_0)$. Note that the equivalent channel matrices $\widetilde{\mathbf{H}}_A^{PNC}$ and $\widetilde{\mathbf{H}}_B^{PNC}$ are $(k+l')$-by-$(k+l')$ square matrices. For such an equivalent MIMO TWRC, efficient techniques can be employed to align the signal directions of the two user into a same set of $k+l'$ directions. This provides a platform to carry out k PNC streams.

So far, we have presented the signal processing techniques used in the proposed space-division scheme to manipulate the uplink channel. The encoding and decoding details of the overall scheme will be described in the next section.

V. AN ACHIEVABLE RATE-REGION OF MIMO TWRC

In this section, we derive an achievable rate-pair of the proposed space-division based PNC scheme. Based on that, we optimize the system parameters to determine the achievable rate-region.

A. *Achievable Rate-Pairs*

1) Complete-Decoding Spatial Streams: The equivalent channel model seen by the complete-decoding spatial streams is given in (29), with the equivalent channel matrices given by $\mathbf{D}_{m,2,2}\mathbf{R}_{m;2,2}$, $m \in \{A, B\}$.

The signal model in (29) is a standard MIMO MAC channel. Let $\mathbf{Q}_m^{CD} = \frac{1}{T}E\left[\mathbf{X}_m^{CD}(\mathbf{X}_m^{CD})^\dagger\right]$ be the input covariance matrix of the complete-decoding spatial steams of user m. Then, the achievable rate-pair of the complete-decoding spatial streams satisfies [24]

$$R_A^{CD} + R_B^{CD} \leq \frac{1}{2}\log\left|\mathbf{I} + \frac{1}{N_0}\sum_{m\in\{A,B\}}\mathbf{D}_{m;2,2}\mathbf{R}_{m;2,2}\mathbf{Q}_m^{CD}\mathbf{R}_{m;2,2}^\dagger\mathbf{D}_{m;2,2}^\dagger\right| \tag{34a}$$

$$R_m^{CD} \leq \frac{1}{2}\log\left|\mathbf{I} + \frac{1}{N_0}\mathbf{D}_{m;2,2}\mathbf{R}_{m;2,2}\mathbf{Q}_m^{CD}\mathbf{R}_{m;2,2}^\dagger\mathbf{D}_{m;2,2}^\dagger\right|, m \in \{A, B\}\,. \tag{34b}$$

2) PNC Spatial Streams: The equivalent channel seen by the PNC streams is given in (32). Recall that $\widetilde{\mathbf{H}}_m^{PNC}$ is a $(k+l')$-by-$(k+l')$ square matrix, and the efficient design of PNC for this case has been discussed in [16]-[18]. Here, we follow the GSVD-based approach in [16], as briefly described below.

Applying the generalized singular-value decomposition (GSVD) [23] to $\widetilde{\mathbf{H}}_m^{PNC}$, we obtain

$$\widetilde{\mathbf{H}}_m^{PNC} = \mathbf{B}\boldsymbol{\Sigma}_m\mathbf{T}_m^\dagger, m \in \{A, B\}\,, \tag{35}$$

where $\mathbf{B} \in \mathbb{C}^{(k+l')\times(k+l')}$ is a nonsingular matrix, $\mathbf{T}_m \in \mathbb{C}^{(k+l')\times(k+l')}$ is an orthogonal matrix, $m \in \{A, B\}$, and $\mathbf{\Sigma}_m \in \mathbb{C}^{(k+l')\times(k+l')}$ is a diagonal matrix with the ith diagonal element denoted by $\sigma_{m;i}$. We further take the QR decomposition to the matrix $\mathbf{B}$, yielding

$$\widetilde{\mathbf{H}}_m^{PNC} = \mathbf{Q}\tilde{\mathbf{R}}\mathbf{\Sigma}_m\mathbf{T}_m^{\dagger}, m \in \{A, B\}\,, \tag{36}$$

where $\tilde{\mathbf{R}} \in \mathbb{C}^{(k+l')\times(k+l')}$ is an upper triangular matrix. The transmit signal $\mathbf{X}_m^{PNC}$ in (32) is designed as

$$\mathbf{X}_m^{PNC} = \mathbf{T}_m\mathbf{\Psi}_m^{1/2}\mathbf{S}_m^{PNC}, m \in \{A, B\}\,, \tag{37}$$

where $\mathbf{\Psi}_m^{1/2} = \text{diag}\big\{\sqrt{\psi_{m;1}}, \sqrt{\psi_{m;2}}, \cdots, \sqrt{\psi_{m;k+l'}}\big\}$ is a diagonal matrix with $\psi_{m;i} \geq 0, i = 1, 2, ..., k+l'$, and $\mathbf{S}_m \in \mathbb{C}^{(k+l')\times T}$ is the signal matrix with each element independent and identically drawn from $\mathcal{N}_c(0, 1)$.

Let R_m^{PNC} be the total rate of the PNC spatial streams of user m. From Theorem 1 in [16], the achievable rate-pair is given by

$$R_m^{PNC} = \sum_{i=1}^{k+l'} \frac{1}{2}\left[\log\left(\frac{I(i)\sigma_{m;i}^2\psi_{m;i}}{\sigma_{A;i}^2\psi_{A;i} + \sigma_{B;i}^2\psi_{B;i}} + \frac{\tilde{r}_{i,i}^2\sigma_{m;i}^2\psi_{m;i}}{N_0}\right)\right]^+, m \in \{A, B\} \tag{38}$$

where $I(i)$ is the indicator function with $I(i) = 1$ for $i = 1$ and $I(i) = 0$ for $i \neq 1$.

3) The Overall Scheme: We now consider the overall achievable rate-pair of the proposed space-division based PNC scheme. Before going into details, we note that the power constraint of user m, i.e., $\frac{1}{T}E\left[\|\mathbf{X}_m\|_F^2\right] \leq P_m$, $m \in \{A, B\}$, can be equivalently expressed as

$$\text{tr}\{\mathbf{Q}_m^{CD}\} + \sum_{i=1}^{k+l'} \psi_{m;i} \leq P_m, m \in \{A, B\}\,. \tag{39}$$

We are now ready to present the following theorem on the achievable rates of the proposed scheme.

Theorem 2: For given $\mathbf{Q}_m^{CD}$, $\mathbf{\Psi}_m$, and $\mathbf{Q}_R$ satisfying (39) and $\text{tr}(\mathbf{Q}_R) \leq P_R$, a rate-pair (R_A, R_B) for the MIMO TWRC is achievable if

$$R_m \leq \min\{R_m^{CD} + R_m^{PNC}, R_m^{DL}\}, m \in \{A, B\}\,, \tag{40}$$

where R_A^{CD} and R_B^{CD} satisfy (34), R_m^{PNC} is given by (38), and R_m^{DL} is given by (4).

Proof: Here we provide a sketch of proof. The overall encoding and decoding process for the proposed scheme is described as follows. The messages of the user m are doubly indexed as (W_m^{CD}, W_m^{PNC}), with $W_m^{CD} \in \{1, 2, ..., 2^{2TR_m^{CD}}\}$ for the complete-decoding spatial streams, and $W_m^{PNC} \in \{1, 2, ..., 2^{2TR_m^{PNC}}\}$ for the PNC spatial streams. Each W_m^{CD} is one-to-one mapped to $\mathbf{X}_m^{CD}$ in (27), and each W_m^{PNC} is one-to-one mapped to $\mathbf{S}_m^{PNC}$ in (37). In the uplink phase, $\mathbf{X}_m^{CD}$ and $\mathbf{X}_m^{PNC} = \mathbf{T}_m \mathbf{\Psi}_m^{1/2} \mathbf{S}_m^{PNC}$ are transmitted via the channel in (27), with the transmit power constrained by (39).

Upon receiving $\mathbf{Y}_R$, the relay first completely decode $\mathbf{X}_A^{CD}$ and $\mathbf{X}_B^{CD}$ based on $\mathbf{Y}_R^{CD}$ in (29), with the achievable rate-pair given in (34). The decoded $\mathbf{X}_A^{CD}$ and $\mathbf{X}_B^{CD}$ are subtracted from $\mathbf{Y}_R^{PNC}$. Let $(\mathbf{s}_{m,i}^{PNC})^T$ be the ith row of $\mathbf{S}_m^{PNC}$. Then, the network-coded PNC spatial streams, i.e., $\tilde{r}_{i,i}\sigma_{A;i}\psi_{A;i}^{1/2}\mathbf{s}_{A,i}^{PNC} + \tilde{r}_{i,i}\sigma_{B;i}\psi_{B;i}^{1/2}\mathbf{s}_{B,i}^{PNC}$, $i = k+l', k+l'-1, ..., 1$, are successively recovered and canceled from $\widetilde{\mathbf{Y}}_R^{PNC}$ in (32), with the achievable rate-pair given in (38). The decoded messages from the complete-decoding streams, together with the network-coded messages from the PNC streams, are then jointly encoded. The new codeword is forwarded to the two users in the downlink phase, with the transmit power constrained by tr$(\mathbf{Q}_R) \leq P_R$. Following the discussions in [16]-[18], the achievable rate-pair of the downlink phase is given by (R_A^{DL}, R_B^{DL}) in (4). This completes the proof. ■

B. Determining Achievable Rate-Region

Now we consider determining the boundary of the achievable rate-region. From (40), the downlink achievable rates are the same as the capacity upper bound in (4). Here, we focus on the uplink rate-region.

The boundary of the uplink rate-region can be determined by solving the following weighted-sum-rate maximization problem:

$$\text{maximize} \quad \sum_{m \in \{A,B\}} w_m \left(R_m^{CD} + R_m^{PNC}\right) \tag{41a}$$

$$\text{subject to} \quad \sum_{j=1}^{k+l'} \psi_{m;j} + \text{tr}\{\mathbf{Q}_m^{CD}\} \leq P_m, \mathbf{Q}_m^{CD} \succeq \mathbf{0}, \psi_{m;i} \geq 0, \text{ for } i = 1, ..., k+l'. \tag{41b}$$

$$R_m^{PNC} = \sum_{i=1}^{k+l'} \frac{1}{2}\left[\log\left(\frac{I(i)\sigma_{m;i}^2\psi_{m;i}}{\sigma_{A;i}^2\psi_{A;i} + \sigma_{B;i}^2\psi_{B;i}} + \frac{\tilde{r}_{i,i}^2\sigma_{m;i}^2\psi_{m;i}}{N_0}\right)\right]^+, \tag{41c}$$

$$R_A^{CD} + R_B^{CD} \leq \frac{1}{2}\log\left|\mathbf{I} + \frac{1}{N_0}\sum_{m\in\{A,B\}} \mathbf{D}_{m;2,2}\mathbf{R}_{m;2,2}\mathbf{Q}_m^{CD}\mathbf{R}_{m;2,2}^{\dagger}\mathbf{D}_{m;2,2}^{\dagger}\right|, \tag{41d}$$

$$R_m^{CD} \leq \frac{1}{2}\log\left|\mathbf{I} + \frac{1}{N_0}\mathbf{D}_{m;2,2}\mathbf{R}_{m;2,2}\mathbf{Q}_m^{CD}\mathbf{R}_{m;2,2}^{\dagger}\mathbf{D}_{m;2,2}^{\dagger}\right|, m \in \{A, B\}. \tag{41e}$$

The above problem involves the optimization of $l', \{\mathbf{p}_i\}_{i=k+1}^{k+l'}, \mathbf{Q}_A^{CD}, \mathbf{Q}_B^{CD}, \{\psi_{A;i}\}_{i=1}^{k+l'}$, and $\{\psi_{B;i}\}_{i=1}^{k+l'}$, as detailed below.

1) Determining the Projection Directions: The optimization of the projection directions $\{\mathbf{p}_i\}_{i=k+1}^{k+l'}$ to maximize the weighted sum-rate is in general difficult to solve. To simplify the problem, we consider the high SNR regime, with the weighted sum-rate given by

$$\begin{aligned}
w_A R_A^{PNC} + w_B R_B^{PNC} &\overset{(a)}{\approx} \frac{1}{2}\sum_{m\in\{A,B\}} w_m \left(\sum_{i=2}^{k+l'} \log\left(\frac{\tilde{r}_{i,i}^2 \sigma_{m;i}^2 \psi_{m;i}}{N_0}\right)\right) \\
&\overset{(b)}{=} \frac{1}{2}\sum_{m\in\{A,B\}} w_m \log\left|\frac{P_m}{N_0 n_m}\tilde{\mathbf{R}}\mathbf{\Sigma}_m\mathbf{\Sigma}_m^{\dagger}\tilde{\mathbf{R}}^{\dagger}\right| \\
&\overset{(c)}{=} \frac{1}{2}\sum_{m\in\{A,B\}} w_m \log\left|\frac{P_m}{N_0 n_m}\tilde{\mathbf{D}}_{m;1,1}\mathbf{R}_{m;1,1}\mathbf{R}_{m;1,1}^{\dagger}\tilde{\mathbf{D}}_{m;1,1}^{\dagger}\right| \\
&\overset{(d)}{=} \frac{1}{2}\sum_{m\in\{A,B\}} \left(w_m \log\left|\frac{P_m}{N_0 n_m}\mathbf{R}_{m;1,1}\mathbf{R}_{m;1,1}^{\dagger}\right| + w_m \log\left|\tilde{\mathbf{D}}_{m;1,1}\tilde{\mathbf{D}}_{m;1,1}^{\dagger}\right|\right) \qquad (42)
\end{aligned}$$

where step (*a*) follows from substituting (38), step (*b*) from the facts that $\tilde{\mathbf{R}}$ is upper-triangular and that equal power allocation is asymptotically optimal (i.e., $\psi_{m;i} = \frac{P_m}{n_m}$), step (*c*) by noting $\tilde{\mathbf{D}}_{m;1,1}\mathbf{R}_{m;1,1} = \widetilde{\mathbf{H}}_m^{PNC} = \mathbf{Q}\tilde{\mathbf{R}}\mathbf{\Sigma}_m\mathbf{T}_m^{\dagger}$ (cf., (32) and (36)), and step (d) by utilizing $|\mathbf{I}+\mathbf{AB}| = |\mathbf{I}+\mathbf{BA}|$. In the above, $\log\left|\tilde{\mathbf{D}}_{m;1,1}\tilde{\mathbf{D}}_{m;1,1}^{\dagger}\right|$ is the only term related to $\mathbf{p}_i$. Recall from (33) that $\tilde{\mathbf{D}}_{m;1,1} = \mathbf{P}^T\mathbf{D}_{m;1,1}$ with $\mathbf{D}_{m;1,1}$ being the principle submatrix of $\mathbf{D}_m$ in (26). Thus, the weighted sum-rate maximization problem over $\{\mathbf{p}_i\}_{i=k+1}^{k+l'}$ can be decoupled into l' independent subproblems as

$$\max_{||\mathbf{p}_i||=1} w_A \log\left(\left|\mathbf{p}_i^{\dagger}\mathbf{e}_{A;i}\right|^2\right) + w_B \log\left(\left|\mathbf{p}_i^{\dagger}\mathbf{e}_{B;i}\right|^2\right), \text{ for } i = k+1, ..., k+l', \qquad (43)$$

where $\mathbf{e}_{A;i}$ and $\mathbf{e}_{B;i}$ are given in (19c). From (13) and the discussions therein, the optimal $\mathbf{p}_i$ to maximize the weighted sum-rate is a real vector given by

$$\mathbf{p}_i = \gamma_i\left(\mathbf{e}_{A;i} + \beta_i \mathbf{e}_{B;i}\right), \text{ for } i = k+1, ..., k+l', \qquad (44)$$

where

$$\beta_i = \frac{1}{2}\left(\sqrt{(\lambda_i - 1)^2\left(1 - \frac{w_B}{w_A}\right)^2 + 4\frac{w_B}{w_A}} - (\lambda_i - 1)\left(1 - \frac{w_B}{w_A}\right)\right), \qquad (45)$$

and γ_i is a scaling factor to ensure $||\mathbf{p}_i|| = 1$.

2) Determining $\mathbf{Q}_A^{CD}$ and $\mathbf{Q}_B^{CD}$: Given $\{\mathbf{p}_i\}$ in (44), the optimization problem in (41) can be decoupled into two separate problems by predetermining the power allocated to the two signal subspaces. Let P_m^{CD} be the power of user m used for the complete-decoding spatial streams. Then, the power for the PNC streams is given by $P_m^{PNC} = P_m - P_m^{CD}, m \in \{A, B\}$. For given P_A^{CD} and P_B^{CD}, the optimal $\mathbf{Q}_A^{CD}$ and $\mathbf{Q}_B^{CD}$ to (41) can be found by solving the following problem:

$$\begin{aligned}
\text{maximize} \quad & w_A R_A^{CD} + w_A R_A^{CD} && \text{(46a)}\\
\text{subject to} \quad & \text{tr}\{\mathbf{Q}_m^{CD}\} \le P_m^{CD}, \mathbf{Q}_m^{CD} \succeq \mathbf{0}, && \text{(46b)}\\
& R_A^{CD} + R_B^{CD} \le \frac{1}{2}\log\left|\mathbf{I} + \frac{1}{N_0}\sum_{m\in\{A,B\}} \mathbf{D}_{m,2,2}\mathbf{R}_{m;2,2}\mathbf{Q}_m^{CD}\mathbf{R}_{m;2,2}^{\dagger}\mathbf{D}_{m,2,2}^{\dagger}\right| && \text{(46c)}\\
& R_m^{CD} \le \frac{1}{2}\log\left|\mathbf{I} + \frac{1}{N_0}\mathbf{D}_{m,2,2}\mathbf{R}_{m;2,2}\mathbf{Q}_m^{CD}\mathbf{R}_{m;2,2}^{\dagger}\mathbf{D}_{m,2,2}^{\dagger}\right|, m \in \{A, B\}\,. && \text{(46d)}
\end{aligned}$$

The above is a standard weighted sum-rate maximization problem for a MIMO multiple-access channel with two users [30]. This problem is convex, and the optimal solution can be numerically obtained using convex programming tools [25].

3) Determining Power Allocation for PNC Streams: Now we consider the optimization of $\{\psi_{A;i}\}_{i=1}^{k+l'}$ and $\{\psi_{B;i}\}_{i=1}^{k+l'}$. Given P_A^{PNC} and P_B^{PNC}, the optimal $\{\psi_{A;i}\}_{i=1}^{k+l'}$ and $\{\psi_{B;i}\}_{i=1}^{k+l'}$ can be determined by solving

$$\begin{aligned}
\text{maximize} \quad & \sum_{m\in\{A,B\}} w_m \left(\sum_{i=1}^{k+l'} \frac{1}{2}\left[\log\left(\frac{I(i)\sigma_{m;i}^2\psi_{m;i}}{\sigma_{A;i}^2\psi_{A;i} + \sigma_{B;i}^2\psi_{B;i}} + \frac{\tilde{r}_{i,i}^2\sigma_{m;i}^2\psi_{m;i}}{N_0}\right)\right]^+\right) && \text{(47a)}\\
\text{subject to} \quad & \sum_{i=1}^{k+l'} \psi_{m;i} \le P_m^{PNC}, \psi_{m;i} \ge 0, \text{ for } i = 1, ..., k + l'. && \text{(47b)}
\end{aligned}$$

A similar problem has been considered in [16], and the optimal solution can be obtained by solving the Karush-Kuhn-Tuchker (KKT) conditions. We omit details here for simplicity.

Base on the above discussions, the weighted sum-rate problem in (41) is numerically solvable given the values of l', P_m^{CD} and P_m^{PNC}, $m \in \{A, B\}$. The optimal l', P_m^{CD} and P_m^{PNC}, $m \in \{A, B\}$ can be found using the exhaustive search. The complexity involved is not significant by noting $P_m^{CD} + P_m^{PNC} = P_m, m \in \{A, B\}$ and the fact that l' is an integer between 0 and l.

VI. ASYMPTOTIC SUM-RATE ANALYSIS

In the preceding section, we have shown the achievable rates of the proposed space-division based network-coding strategy for MIMO TWRCs. In general, it is difficult to represent the achievable rate of the optimized space-division based scheme in a closed-form. Thus, it is not easy to evaluate the gap between the achievable rate of the proposed scheme and the capacity upper bound of the MIMO TWRC. In this section, we derive a closed-form expression for the asymptotic sum-rate of the proposed strategy in the high SNR regime.

A. Asymptotic Sum-Rate as SNR $\to \infty$

Here, we analyze the uplink achievable sum-rate

$$R^{SD} = \sum_{m \in \{A,B\}} R_m^{CD} + R_m^{PNC} \tag{48}$$

as the SNRs, i.e., $\frac{P_A}{N_0}$ and $\frac{P_B}{N_0}$, tend to infinity. It is known that, in the high SNR regime, equal power allocation is asymptotically optimal. Then, the upper bound of the uplink sum-rate of the MIMO TWRC is given by (cf., (4))

$$R^{UL} \approx \frac{1}{2} \sum_{m \in \{A,B\}} \log \left| \mathbf{I}_{n_R} + \frac{P_m}{N_0 n_m} \mathbf{H}_m \mathbf{H}_m^{\dagger} \right| \tag{49}$$

where "$x \approx y$" means

$$\lim_{SNR \longrightarrow \infty} (x - y) = 0.$$

Now, we present the following theorem on the asymptotic sum-rate of the proposed scheme. Denote by R^{SD} the uplink achievable sum-rate of the proposed space-division scheme.

Theorem 3: For a given l', the uplink achievable sum-rate of the proposed space-division scheme satisfies

$$\lim_{SNR \longrightarrow \infty} R^{UL} - R^{SD} = \Delta^{SD} \tag{50a}$$

where

$$\Delta^{SD} \triangleq -\log \prod_{i=k+1}^{k+l'} \frac{\lambda_i}{2} - \log \prod_{i=k+l'+1}^{k+l} \sqrt{\lambda_i (2 - \lambda_i)} \geq 0. \tag{50b}$$

The proof of Theorem 3 can be found in Appendix B. Notice that the first term in (50b), i.e., $-\log \prod_{i=k+1}^{k+l'} \frac{\lambda_i}{2}$, is the rate loss incurred by the PNC spatial streams, and the second term, i.e., $\log \prod_{i=k+l'+1}^{k+l} \sqrt{\lambda_i (2 - \lambda_i)}$, is that incurred by the complete-decoding spatial streams.

Remark 5: For the case of $n_A, n_B \geq n_R$, we have $l = 0$ and $\lambda_i = 2$ for $i = 1, ..., k$. (See Remark (4).) Then, from (50b), we have $\Delta^{SD} = 0$, which means that the scheme is asymptotically optimal. This agrees with the fact that our proposed space-division scheme reduces to the GSVD scheme which is indeed asymptotically optimal in the high SNR regime [16].

Corollary 3: The optimal l' to minimize the rate gap Δ^{SD} in (50b) satisfies

$$2 > \lambda_{k+1} \geq ... \geq \lambda_{k+l'} \geq \frac{8}{5} > \lambda_{k+l'+1} \geq ... \geq \lambda_{k+l} > 1. \tag{51}$$

With this choice of l', the asymptotic rate gap Δ^{SD} is at most $l \log(5/4)$ bits, which occurs when $\lambda_{k+1} = \lambda_{k+2} = ... = \lambda_{k+l} = \frac{8}{5}$.

Remark 6: From the above corollary, the asymptotic gap to the sum-capacity upper bound is $l \log(5/4)$ bits for the worst case. Noting $l \leq n_m, m \in \{A, B\}$, we see that the gap is at most $\min\{n_A, n_B\} \log(5/4)$ bits, or $\frac{1}{2} \log(5/4) \approx 0.161$ bits per user-antenna.

B. Average Sum-Rate via Large-System Analysis

In this subsection, we investigate the statistical average of the rate gap Δ^{SD} in fading channels. To this end, the distribution of $\{\lambda_i\}$, i.e., the eigenvalues of $\mathbf{U}_A \mathbf{U}_A^\dagger + \mathbf{U}_B \mathbf{U}_B^\dagger$, is required. However, such a distribution is difficult to obtain in general. Here, we employ the large-system analysis to find an approximation of the distribution of $\{\lambda_i\}$. The distribution obtained in this way becomes exact as the number of antennas in the system is large.

We assume Rayleigh fading, in which the channel coefficients are i.i.d. circularly symmetric complex Gaussian random variables. Then, the matrices $\mathbf{U}_A$ and $\mathbf{U}_B$ in (17) are truncated uniformly distributed unitary matrices, or alternatively, are asymptotically free random matrices [26]. Thus, we can use the theory of free probabilities to derive the asymptotic eigenvalue distribution (a.e.d.) of $\mathbf{U}_A \mathbf{U}_A^\dagger + \mathbf{U}_B \mathbf{U}_B^\dagger$ as n_R tends to infinity, with the result given in the lemma below. Define $\eta_m \triangleq \frac{n_m}{n_R}, m \in \{A, B\}$.

Lemma 1: As $n_R \to \infty$ with $\frac{n_A}{n_R} \to \eta_A$ and $\frac{n_B}{n_R} \to \eta_B$, the a.e.d. of $\mathbf{U}_A \mathbf{U}_A^\dagger + \mathbf{U}_B \mathbf{U}_B^\dagger$ is given by

$$\begin{aligned} \mathcal{F}(\lambda; \eta_A, \eta_B) &= [1 - \eta_A - \eta_B]^+ \delta(\lambda) + |\eta_A - \eta_B| \delta(\lambda - 1) + [\eta_A + \eta_B - 1]^+ \delta(\lambda - 2) \\ &\quad + \frac{1}{\pi} \mathrm{Im}\left[\frac{\sqrt{(1 - \eta_A - \eta_B)^2 - \left(2\lambda - \lambda^2\right)\left(1 - \left(\frac{\eta_A - \eta_B}{\lambda - 1}\right)^2\right)}}{2\lambda - \lambda^2} \right] \end{aligned} \tag{52}$$

where $\delta(\cdot)$ is a Dirac delta function and $\mathrm{Im}[\cdot]$ is the imaginary part of a complex number.

The proof of the above lemma can be found in Appendix C. As $n_R \to \infty$, we see that for $\eta_A + \eta_B \geq 1$, the portion of eigenvalues $\{\lambda_i\}$ equal to 2 is given by $\eta_A + \eta_B - 1$. This portion corresponds to the dimension of the common space $\mathcal{S}_{A\|B}$ of $\mathbf{H}_{AR}$ and $\mathbf{H}_{BR}$. In addition, for $\eta_A \neq \eta_B$, the portion of eigenvalues $\{\lambda_i\}$ equal to 1 is given by $|\eta_A - \eta_B|$. This portion corresponds to the dimension of $\mathcal{S}_{A\perp B}$ if $\eta_A \geq \eta_B$ or the dimension of $\mathcal{S}_{B\perp A}$ if $\eta_A < \eta_B$.

We are now ready to present the following asymptotic result.

Theorem 4: As $n_R \to \infty$ with $\frac{n_A}{n_R} \to \eta_A$ and $\frac{n_B}{n_R} \to \eta_B$, the gap to the capacity upper bound satisfies

$$r^{SD} \triangleq \lim_{n_R\to\infty} \frac{\Delta^{SD}}{n_R} = -\left(\int_1^{\frac{8}{5}} \log\sqrt{\lambda(2-\lambda)} + \int_{\frac{8}{5}}^{2} \log\frac{\lambda}{2}\right)\mathcal{F}(\lambda;\eta_A,\eta_B)d\lambda. \tag{53}$$

Proof: The a.e.d. of λ_i is given by Lemma 1. Then, letting n_R tends to infinity in (50b), we immediately obtain the theorem. ■

Let $\overline{R}^{UL}$ be the average sum-capacity upper bound. Then, for a large n_R, the average sum-rate of the proposed SD scheme can be first-order approximated as

$$\overline{R}^{SD} = \overline{R}^{UL} - n_R r^{SD} \tag{54}$$

with r^{SD} given in (53).

We next study the symmetric case that the two users are equipped with the same number of antennas, i.e., $\eta_A = \eta_B = \eta$.

Corollary 4: For $0 \leq \eta \leq \frac{1}{10}$,

$$r^{SD} = -\int_1^{\lambda^*(\eta)} \log\sqrt{\lambda(2-\lambda)}\mathcal{G}(\lambda;\eta)d\lambda; \tag{55a}$$

for $\frac{1}{10} < \eta \leq 1$,

$$r^{SD} = -\left(\int_1^{\frac{8}{5}} \log\sqrt{\lambda(2-\lambda)} + \int_{\frac{8}{5}}^{\lambda^*(\eta)} \log\frac{\lambda}{2}\right)\mathcal{G}(\lambda;\eta)d\lambda, \tag{55b}$$

where $\lambda^*(\eta) = 1 + \sqrt{1-(1-2\eta)^2}$ and

$$\mathcal{G}\left(\lambda;\eta\right) = \frac{1}{\pi}\frac{\sqrt{\left(2\lambda-\lambda^2\right)-(1-2\eta)^2}}{2\lambda-\lambda^2}. \tag{55c}$$

Proof: Letting $\eta_A = \eta_B = \eta$, we obtain that $\mathcal{F}\left(\lambda;\eta_A,\eta_B\right) = \mathcal{G}\left(\lambda;\eta\right)$ for $1 < \lambda < \lambda^*$, and $\mathcal{F}\left(\lambda;\eta_A,\eta_B\right) = 0$ for $\lambda^* < \lambda < 2$. In addition, $\lambda^*(\eta) = \frac{8}{5}$ implies $\eta = \frac{1}{10}$. Based on these facts and Theorem 4, we obtain the corollary. ■

Remark 7: From the above, we see that, if $\eta \leq \frac{1}{10}$, the probability of $\lambda_i > \frac{8}{5}$ approaches zero as $n_R \to \infty$, implying that complete decoding achieves a higher rate than PNC for all spatial streams.

Corollary 5: The asymptotic normalized rate gap r^{SD} in (53) is maximized at $\eta_A = \eta_B = 1/2$, with the maximum given by

$$-\frac{1}{\pi}\left(\int_{1}^{\frac{8}{5}} \frac{\log\sqrt{\lambda(2-\lambda)}}{\sqrt{2\lambda-\lambda^2}}d\lambda + \int_{\frac{8}{5}}^{2} \frac{\log\frac{\lambda}{2}}{\sqrt{2\lambda-\lambda^2}}d\lambda\right) \approx 0.053 \text{ bit.} \tag{56}$$

Proof: We first consider optimizing η_A and η_B under the constraint of $\eta_A + \eta_B = 2\eta$. From (52), we see that, for any $\lambda \in (1, 2)$, $\mathcal{F}(\lambda; \eta_A, \eta_B)$ is maximized at $\eta_A = \eta_B = \eta$, and so is r^{SD}.

What remains is to optimize η. From (55c), $\mathcal{G}(\lambda; \eta)$ is maximized at $\eta = 1/2$. Therefore, r^{SD} is maximized at $\eta = 1/2$, which completes the proof. ■

Fig. 3 illustrates the function of the normalized asymptotic rate gap r^{SD} against η. From Fig. 3, this rate gap is maximized at $\eta = 1/2$, which verifies Corollary 5. Also, this rate gap vanishes as η tends to 0, implying that, for any fixed $n_A = n_B$, the proposed space-division scheme can achieve the asymptotic capacity as n_R tends to infinity. Moreover, this rate gap vanishes as η tends to 1. This agrees with the fact that, for $\eta \geq 1$, or equivalently, $n_A = n_B \geq n_R$, the proposed space-division based scheme reduces to the GSVD scheme in [16].

VII. NUMERICAL RESULTS

In this section, we provide numerical results to evaluate the performance of the proposed space-division based network-coding strategy for MIMO TWRCs. The results presented below are obtained by averaging over 1,0000 random channel realizations. Rayleigh-fading is assumed, i.e., the coefficients in the channel matrices are independently and identically drawn from $\mathcal{N}_c(0, 1)$.

We first present the numerical results for a MIMO TWRC of $n_A = n_B = 2$ and $n_R = 4$ in Fig. 4. The sum-capacity upper bound (UB), the proposed space-division (SD) scheme, the GSVD scheme in [16] and the complete-decoding scheme in [17] are included for comparison. We see that, at a relatively high SNR, e.g., SNR = 25 dB, the rate gap between the proposed SD scheme and the sum-capacity upper bound is about 0.15 bit/channel-use, which is almost unnoticeable. We also plot the high-SNR analytical result in (54) of the proposed SD scheme. We observe that our analytical result are very tight for SNRs greater than 10 dB.

From this figure, it is clear that the proposed SD scheme significantly outperforms the other schemes in the entire SNR range of interest. For example, at the rate of 14 bits per channel use, the proposed SD scheme outperforms the complete-decoding and GSVD schemes by more than 2.4 dB. The slope of the achievable sum-rate curve is parallel to that of the capacity upper bound, which implies that the proposed SD scheme achieves full multiplexing gain.

In Fig. 5, we present the numerical results for a MIMO TWRC of $n_A = n_B = 2$ and $n_R = 3$. The same set of rate curves from simulation as in Fig. 4 are included for comparison. Again, we see that the gap between the sum-rate of the proposed SD scheme and the sum-capacity upper bound is almost unnoticeable at a relatively high SNR, e.g., greater than 15 dB. The proposed SD scheme outperforms its counterparts throughout the SNR range of interest.

In Figures 6 and 7, we show the scaling effect of the antennas on the average achievable sum-rates. We see that the asymptotic rate gap between the proposed SD scheme and the sum-capacity upper bound increases linearly as the increase of n_R for fixed η_A and η_B. For example, for the case of $\eta_A = \eta_B = 1/2$ in Fig. 6, the rate gap at SNR = 25 dB is 0.14 bits per channel use for $n_R = 4$; 0.29 bits per channel use for $n_R = 6$; and 0.40 bits per channel use for $n_R = 8$. These numerical results agree well with the asymptotic results in Corollaries 4 and 5.

In Fig. 8, we show the achievable rate-region of the proposed SD scheme. The capacity-region outer bound and the achievable rate-region of the complete-decoding scheme are also included for comparison. From Fig. 8, the difference between the achievable rate-region of the proposed SD scheme and the capacity region outer bound is negligible for a relatively high SNR. We also see that the proposed SD scheme can achieve rate-pairs that cannot be achieved by the complete-decoding scheme.

VIII. CONCLUSION

In this paper, we developed a new joint channel decomposition for MIMO TWRCs. Based on that, we proposed a space-division based network-coding scheme with the achievable sum-rate within $\frac{1}{2}\log(5/4) \approx 0.161$ bit per user-antenna of the capacity upper bound in the high SNR regime. We also show that, for Rayleigh-fading MIMO TWRCs, the average gap between the achievable rate of the proposed scheme and the capacity upper bound is no more than 0.053 bit per relay-antenna in the high SNR regime. We remark that this marginal gap is due to the fact that the complete-decoding and PNC strategies, collectively, fail to achieve the asymptotic capacity upper bound, even for the case of single-antenna users. To completely remove this gap, more advanced multi-dimension PNC relaying strategies may be required. Moreover, in this paper, channel state information is assumed to be globally known by both the transmitter and receiver sides. It is of theoretical, and more practical, interests to investigate how to efficiently communicate over MIMO TWRCs where only the receiver-side channel state information is available. We will look into these problems in our future research.

APPENDIX A

PROOF OF THEOREM 1

Here we prove Theorem 1. Let λ_i be an eigenvalue of $\mathbf{U}_A\mathbf{U}_A^\dagger + \mathbf{U}_B\mathbf{U}_B^\dagger$ and $\mathbf{u}_i$ be the corresponding unit-length eigenvector satisfying

$$\left(\mathbf{U}_A\mathbf{U}_A^\dagger + \mathbf{U}_B\mathbf{U}_B^\dagger\right)\mathbf{u}_i = \lambda_i\mathbf{u}_i. \tag{57}$$

We are interested in four cases of λ_i: (a) $\lambda_i = 2$; (b) $1 < \lambda_i < 2$; (c) $\lambda_i = 1$; and (d) $0 < \lambda_i < 1$.

For case (a), $\lambda_i = 2$ implies that

$$\mathbf{U}_A\mathbf{U}_A^\dagger\mathbf{u}_i = \mathbf{u}_i \text{ and } \mathbf{U}_B\mathbf{U}_B^\dagger\mathbf{u}_i = \mathbf{u}_i.$$

Thus, $\mathbf{u}_i$ lies in the common space of $\mathcal{C}(\mathbf{U}_A)$ and $\mathcal{C}(\mathbf{U}_B)$.

For case (c), we have

$$\mathbf{U}_A\mathbf{U}_A^\dagger\mathbf{u}_i = \mathbf{u}_i \text{ and } \mathbf{U}_B\mathbf{U}_B^\dagger\mathbf{u}_i = \mathbf{0} \tag{58a}$$

or

$$\mathbf{U}_A\mathbf{U}_A^\dagger\mathbf{u}_i = \mathbf{0} \text{ and } \mathbf{U}_B\mathbf{U}_B^\dagger\mathbf{u}_i = \mathbf{u}_i. \tag{58b}$$

We next show that the eigenvalues in case (b) and case (d) appear in a pair-wise manner. Denote

$$\mathbf{l}_{m;i} = \mathbf{U}_m\left(\mathbf{U}_m^\dagger\mathbf{U}_m\right)^{-1}\mathbf{U}_m^\dagger\mathbf{u}_i = \mathbf{U}_m\mathbf{U}_m^\dagger\mathbf{u}_i. \tag{59}$$

Note that $\mathbf{l}_{m;i}$ is the projection of vector $\mathbf{u}_i$ onto the column space of $\mathbf{U}_m$. From (57), we obtain

$$\mathbf{u}_i = \frac{1}{\lambda_i}\left(\mathbf{l}_{A;i} + \mathbf{l}_{B;i}\right). \tag{60}$$

The above implies that $\mathbf{u}_i$, $\mathbf{l}_{A;i}$ and $\mathbf{l}_{B;i}$ lie on the same two-dimension plane (denoted by $\mathcal{S}_i$). We have the following facts.

Lemma 2: For any λ_i in case (b), the corresponding $\mathbf{u}_i$ is the angular bisector of $\mathbf{l}_{A;i}$ and $\mathbf{l}_{B;i}$, i.e.

$$\|\mathbf{l}_{A;i}\|^2 = \mathbf{u}_i^\dagger \mathbf{l}_{A;i} = \mathbf{u}_i^\dagger \mathbf{l}_{B;i} = \|\mathbf{l}_{B;i}\|^2 . \tag{61}$$

Proof: To prove the lemma, we first multiply both sides of (57) by $\mathbf{U}_A\mathbf{U}_A^\dagger$. Then, after some straightforward manipulations, we obtain

$$(\lambda_i - 1)\,\mathbf{U}_A\mathbf{U}_A^\dagger\mathbf{u}_i = \mathbf{U}_A\mathbf{U}_A^\dagger\mathbf{U}_B\mathbf{U}_B^\dagger\mathbf{u}_i. \tag{62}$$

Similarly, we have

$$(\lambda_i - 1)\,\mathbf{U}_B\mathbf{U}_B^\dagger\mathbf{u}_i = \mathbf{U}_B\mathbf{U}_B^\dagger\mathbf{U}_A\mathbf{U}_A^\dagger\mathbf{u}_i. \tag{63}$$

Then,

$$\begin{aligned}\mathbf{u}_i^\dagger\mathbf{l}_{A;i} &\overset{(a)}{=} \mathbf{u}_i^\dagger\mathbf{U}_A\mathbf{U}_A^\dagger\mathbf{u}_i \overset{(b)}{=} \frac{1}{\lambda_i - 1}\mathbf{u}_i^\dagger\mathbf{U}_A\mathbf{U}_A^\dagger\mathbf{U}_B\mathbf{U}_B^\dagger\mathbf{u}_i\\ &\overset{(c)}{=} \frac{1}{\lambda_i - 1}\mathbf{u}_i^\dagger\mathbf{U}_B\mathbf{U}_B^\dagger\mathbf{U}_A\mathbf{U}_A^\dagger\mathbf{u}_i \overset{(d)}{=} \mathbf{u}_i^\dagger\mathbf{U}_B\mathbf{U}_B^\dagger\mathbf{u}_i \overset{(e)}{=} \mathbf{u}_i^\dagger\mathbf{l}_{B;i}\end{aligned}$$

where step (a) follows from (59), (b) from (62), (c) from the fact that the Hermitian transpose of a real-valued scalar is itself, (d) from (63), and (e) again from (59). From (59), the projection of $\mathbf{u}_i$ onto $\mathbf{l}_{m;i}$ is just $\mathbf{l}_{m;i}$. Thus, $\|\mathbf{l}_{m;i}\|^2 = \mathbf{u}_i^\dagger\mathbf{l}_{m;i}$, which completes the proof. ■

Lemma 3: For any $\lambda_i \in (1,2)$ (as in case (b)), $\lambda_i' = 2 - \lambda_i$ is also an eigenvalue of $\mathbf{U}_A\mathbf{U}_A^\dagger + \mathbf{U}_B\mathbf{U}_B^\dagger$, and the corresponding unit-length eigenvector is given by

$$\mathbf{u}_i' = \frac{1}{\sqrt{\lambda_i\lambda_i'}}\left(\mathbf{l}_{A;i} - \mathbf{l}_{B;i}\right). \tag{64}$$

Proof: By definition, we have

$$\begin{aligned}&\left(\mathbf{U}_A\mathbf{U}_A^\dagger + \mathbf{U}_B\mathbf{U}_B^\dagger\right)\mathbf{u}_i'\\ &\overset{(a)}{=} \frac{1}{\sqrt{\lambda_i\lambda_i'}}\left(\mathbf{U}_A\mathbf{U}_A^\dagger + \mathbf{U}_B\mathbf{U}_B^\dagger\right)(\mathbf{l}_{A;i} - \mathbf{l}_{B;i})\\ &\overset{(b)}{=} \frac{1}{\sqrt{\lambda_i\lambda_i'}}\left(\mathbf{U}_A\mathbf{U}_A^\dagger\mathbf{u}_i + (\lambda_i - 1)\,\mathbf{U}_B\mathbf{U}_B^\dagger\mathbf{u}_i - (\lambda_i - 1)\,\mathbf{U}_A\mathbf{U}_A^\dagger\mathbf{u}_i - \mathbf{U}_B\mathbf{U}_B^\dagger\mathbf{u}_i\right)\\ &= \frac{\lambda_i'}{\sqrt{\lambda_i\lambda_i'}}(\mathbf{l}_{A;i} - \mathbf{l}_{B;i}) = \lambda_i'\mathbf{u}_i'\end{aligned} \tag{65}$$

where step (a) follows from (64), and step (b) from (59), (62) and (63).

What remains is to show that $\|\mathbf{u}_i'\| = 1$. To see this, we left-multiply both sides of (57) by $\mathbf{u}_i^\dagger$, yielding

$$\|\mathbf{l}_{A;i}\|^2 + \|\mathbf{l}_{B;i}\|^2 = \lambda_i. \tag{66}$$

Together with (61), we obtain

$$\|\mathbf{l}_{A;i}\|^2 = \|\mathbf{l}_{B;i}\|^2 = \frac{\lambda_i}{2}. \tag{67}$$

Moreover, left multiplying (62) and (63) respectively by $\mathbf{u}_i^\dagger$ and plugging in (59), we obtain

$$\mathbf{l}_{A;i}^\dagger \mathbf{l}_{B;i} = (\lambda_i - 1)\|\mathbf{l}_{A;i}\|^2 = (\lambda_i - 1)\|\mathbf{l}_{B;i}\|^2 = \mathbf{l}_{B;i}^\dagger \mathbf{l}_{A;i}. \tag{68}$$

Then

$$\begin{aligned}
\mathbf{u}_i'^\dagger \mathbf{u}_i' &= \frac{1}{\lambda_i \lambda_i'} \left(\mathbf{l}_{A;i} - \mathbf{l}_{B;i}\right)^\dagger \left(\mathbf{l}_{A;i} - \mathbf{l}_{B;i}\right) \\
&= \frac{1}{\lambda_i \lambda_i'} \left(\|\mathbf{l}_{A;i}\|^2 - \mathbf{l}_{A;i}^\dagger \mathbf{l}_{B;i} - \mathbf{l}_{B;i}^\dagger \mathbf{l}_{A;i} + \|\mathbf{l}_{B;i}\|^2\right) \\
&\overset{(a)}{=} \frac{1}{\lambda_i \lambda_i'} \left(\lambda_i - (\lambda_i - 1)\|\mathbf{l}_{A;i}\|^2 - (\lambda_i - 1)\|\mathbf{l}_{B;i}\|^2\right) \\
&\overset{(b)}{=} 1
\end{aligned} \tag{69}$$

where step (a) follows from (67) and (68), and step (b) from (67) and the fact of $\lambda_i' = 2 - \lambda_i$. This completes the proof. ■

Lemma 4: The subspace $\mathcal{S}_i$ spanned by $\mathbf{l}_{A;i}$ and $\mathbf{l}_{B;i}$ is orthogonal to $\mathcal{S}_j$, for any $j \neq i$.

Proof: From (60) and (64), we see that both $\mathbf{u}_i$ and $\mathbf{u}_i'$ lie on the plane $\mathcal{S}_i$. As $\mathbf{u}_i$ and $\mathbf{u}_i'$ are orthogonal to each other, $\mathcal{S}_i$ is spanned by $\mathbf{u}_i$ and $\mathbf{u}_i'$. Then, the lemma holds straightforwardly by noting the orthogonality between the eigenvectors. ■

Now we give an overall picture of the eigenvalues and eigenvectors of $\mathbf{U}_A\mathbf{U}_A^\dagger + \mathbf{U}_B\mathbf{U}_B^\dagger$. Denote the k eigenvalues in case (a) by $\lambda_1, \cdots, \lambda_k$, and the corresponding orthogonal eigenvectors by $\mathbf{u}_1, \cdots, \mathbf{u}_k$. Also denote the l eigenvalues in case (b) by $\lambda_{k+1}, \cdots, \lambda_{k+l}$ in the descending order, and the corresponding eigenvectors by $\mathbf{u}_{k+1}, \cdots, \mathbf{u}_{k+l}$. As the eigenvalues in (b) and (d) appears in a pair-wise manner, we further denote the l eigenvalues in case (d) by $\lambda_{k+1}', \cdots, \lambda_{k+l}'$ in the descending order, and the corresponding eigenvectors by $\mathbf{u}'_{k+1}, \cdots, \mathbf{u}'_{k+l}$. Moreover, we denote the d_A orthogonal eigenvectors in case (c.1) by $\mathbf{u}_{k+l+1}, \cdots, \mathbf{u}_{k+l+d_A}$, and the d_B orthogonal eigenvectors in case (c.2) by $\mathbf{u}_{k+l+d_A+1}, \cdots, \mathbf{u}_{k+l+d_A+d_B}$. Let

$$\mathbf{U} = \left[\mathbf{u}_1, \cdots, \mathbf{u}_k, \mathbf{u}_{k+1}, \mathbf{u}'_{k+1}, \cdots, \mathbf{u}_{k+l}, \mathbf{u}'_{k+l}, \mathbf{u}_{k+l+1}, ..., \mathbf{u}_{k+l+d_A+d_B}\right]. \tag{70}$$

It can be readily verified that $\mathbf{U}$ is an orthonormal matrix satisfying $\mathbf{U}^\dagger\mathbf{U} = \mathbf{I}_{n_A+n_B-k}$. Define

$$\mathbf{U}'_A = \left[\mathbf{u}_1, \cdots, \mathbf{u}_k, \frac{\mathbf{l}_{A;k+1}}{\|\mathbf{l}_{A;k+1}\|}, \cdots, \frac{\mathbf{l}_{A;k+l}}{\|\mathbf{l}_{A;k+l}\|}, \mathbf{u}_{k+l+1}, ..., \mathbf{u}_{k+l+d_A}\right] \tag{71a}$$

and

$$\mathbf{U}'_B = \left[\mathbf{u}_1, \cdots, \mathbf{u}_k, \frac{\mathbf{l}_{B;k+1}}{\|\mathbf{l}_{B;k+1}\|}, \cdots, \frac{\mathbf{l}_{B;k+l}}{\|\mathbf{l}_{B;k+l}\|}, \mathbf{u}_{k+l+d_A+1}, ..., \mathbf{u}_{k+l+d_A+d_B}\right]. \tag{71b}$$

In the above, $\mathbf{u}_1, \cdots, \mathbf{u}_k$ are the eigenvectors in case (a); $\mathbf{u}_{k+l+1}, ..., \mathbf{u}_{k+l+d_A}$ are the eigenvectors in case (c) satisfying $\mathbf{U}_A\mathbf{U}_A^\dagger\mathbf{u}_i = \mathbf{u}_i$, for $i = k+l+1, ..., k+l+d_A$; $\mathbf{u}_{k+l+d_A+1}, \cdots, \mathbf{u}_{k+l+d_A+d_B}$ are the eigenvectors in case (c) satisfying $\mathbf{U}_B\mathbf{U}_B^\dagger\mathbf{u}_i = \mathbf{u}_i$, for $i = k+l+d_A+1, ..., k+l+d_A+d_B$.

Then, from Lemmas 3 and 4, it can be verified that $\mathbf{D}_m$ in (19a) satisfies

$$\mathbf{U}'_m = \mathbf{U}\mathbf{D}_m, m \in \{A, B\}. \tag{72}$$

From Lemma 3 and the fact that $\mathbf{l}_{m;i} \in \mathcal{S}_i$ for $i = k+1, \cdots, k+l$, the columns of $\mathbf{U}'_m$ are orthonormal. Together with the fact that all columns of $\mathbf{U}'_m$ lie in the columnspace of $\mathbf{U}_m$ (and so in the columnspace of $\mathbf{H}_m$), we see that $\mathbf{H}_m$ and $\mathbf{U}'_m$ share the same columnspace. Thus, there exists an n_m-by-n_m square matrix $\mathbf{G}_m$ such that

$$\mathbf{H}_{mR} = \mathbf{U}'_m\mathbf{G}_m. \tag{73}$$

Combining (72) and (73), we obtain

$$\mathbf{H}_{mR} = \mathbf{U}\mathbf{D}_m\mathbf{G}_m \tag{74}$$

which completes the proof of Theorem 1.

APPENDIX B

PROOF OF THEOREM 3

We first consider the sum-rate upper bound:

$$\begin{aligned} R^{UL} &\overset{(a)}{\approx} \frac{1}{2}\sum_{m\in\{A,B\}} \log\left|\mathbf{I}_{n_R}+\frac{P_m}{N_0 n_m}\mathbf{U}\mathbf{D}_m\mathbf{R}_m\mathbf{R}_m^{\dagger}\mathbf{D}_m^{\dagger}\mathbf{U}^{\dagger}\right| \\ &\overset{(b)}{=} \frac{1}{2}\sum_{m\in\{A,B\}} \log\left|\mathbf{I}_{n_m}+\frac{P_m}{N_0 n_m}\mathbf{R}_m\mathbf{R}_m^{\dagger}\right| \\ &\overset{(c)}{\approx} \frac{1}{2}\sum_{m\in\{A,B\}} \log\left|\frac{P_m}{N_0 n_m}\mathbf{R}_m\mathbf{R}_m^{\dagger}\right| \end{aligned} \tag{75}$$

where step (*a*) follows by substituting (24) into (49), step (*b*) follows from the facts that $\mathbf{D}_m^{\dagger}\mathbf{U}^{\dagger}\mathbf{U}\mathbf{D}_m = \mathbf{I}_{n_m}$ and $|\mathbf{I}+\mathbf{AB}| = |\mathbf{I}+\mathbf{BA}|$, and step (*c*) utilizes the fact that $\mathbf{R}_m$ is a square matrix.

Now we consider the achievable sum-rate of the proposed space-division scheme. For notational simplicity, let $\mathbf{H}_m^{CD} = \mathbf{D}_{m;2,2}\mathbf{R}_{m;2,2}$, $m \in \{A, B\}$. From (34), the sum-rate of the complete-decoding spatial streams can be expressed as

$$\begin{aligned} R_A^{CD}+R_B^{CD} &\overset{(a)}{=} \frac{1}{2}\log\left|\mathbf{I}+\sum_{m\in\{A,B\}}\frac{P_m}{N_0 n_m}\mathbf{H}_m^{CD}(\mathbf{H}_m^{CD})^{\dagger}\right| \\ &\overset{(b)}{=} \frac{1}{2}\log\left|\mathbf{I}+\frac{P_A}{N_0 n_A}\mathbf{H}_A^{CD}(\mathbf{H}_A^{CD})^{\dagger}\right| + \frac{1}{2}\log\frac{\left|\mathbf{I}+\sum_{m\in\{A,B\}}\frac{P_m}{N_0 n_m}\mathbf{H}_m^{CD}(\mathbf{H}_m^{CD})^{\dagger}\right|}{\left|\mathbf{I}+\frac{P_A}{N_0 n_A}\mathbf{H}_A^{CD}(\mathbf{H}_A^{CD})^{\dagger}\right|} \\ &\overset{(c)}{\approx} \frac{1}{2}\log\left|\frac{P_A}{N_0 n_A}\mathbf{R}_{A;2,2}\mathbf{R}_{A;2,2}^{\dagger}\right| + \frac{1}{2}\log\left|\frac{P_B}{N_0 n_B}(\mathbf{H}_B^{CD})^{\dagger}\left(\mathbf{I}+\frac{P_A}{N_0 n_A}\mathbf{H}_A^{CD}(\mathbf{H}_A^{CD})^{\dagger}\right)^{-1}\mathbf{H}_B^{CD}\right| \\ &\overset{(d)}{=} \sum_{m\in\{A,B\}}\frac{1}{2}\log\left|\frac{P_m}{N_0 n_m}\mathbf{R}_{m;2,2}\mathbf{R}_{m;2,2}^{\dagger}\right| + \frac{1}{2}\log\left|\mathbf{D}_{B;2,2}^{\dagger}\left(\mathbf{I}+\frac{P_A}{N_0 n_A}\mathbf{H}_A^{CD}(\mathbf{H}_A^{CD})^{\dagger}\right)^{-1}\mathbf{D}_{B;2,2}\right| \end{aligned}$$

where step (*a*) utilizes the fact that equal power allocation is asymptotically optimal, and step (d) follows by substituting $\mathbf{H}_B^{CD} = \mathbf{D}_{B;2,2}\mathbf{R}_{B;2,2}$. Applying the matrix inversion lemma to $\left(\mathbf{I}+\frac{P_A}{N_0 n_A}\mathbf{H}_A^{CD}(\mathbf{H}_A^{CD})^{\dagger}\right)^{-1}$, we further obtain

$$\begin{aligned}
R_A^{CD}+R_B^{CD} &= \sum_{m\in\{A,B\}} \frac{1}{2}\log\left|\frac{P_m}{N_0 n_m}\mathbf{R}_{m;2,2}\mathbf{R}_{m;2,2}^{\dagger}\right| \\
&\quad + \frac{1}{2}\log\left|\mathbf{I}-\frac{P_A}{N_0 n_A}\mathbf{D}_{B;2,2}^{\dagger}\mathbf{H}_A^{CD}\left(\mathbf{I}+\frac{P_A}{N_0 n_A}(\mathbf{H}_A^{CD})^{\dagger}\mathbf{H}_A^{CD}\right)^{-1}(\mathbf{H}_A^{CD})^{\dagger}\mathbf{D}_{B;2,2}\right| \\
&\overset{(a)}{\approx} \sum_{m\in\{A,B\}} \frac{1}{2}\log\left|\frac{P_m}{N_0 n_m}\mathbf{R}_{m;2,2}\mathbf{R}_{m;2,2}^{\dagger}\right| + \frac{1}{2}\log\left|\mathbf{I}-\mathbf{D}_{B;2,2}^{\dagger}\mathbf{D}_{A;2,2}\mathbf{D}_{A;2,2}^{\dagger}\mathbf{D}_{B;2,2}\right| \\
&\overset{(b)}{=} \sum_{m\in\{A,B\}} \frac{1}{2}\log\left|\frac{P_m}{N_0 n_m}\mathbf{R}_{m;2,2}\mathbf{R}_{m;2,2}^{\dagger}\right| + \frac{1}{2}\log\prod_{i=k+l'+1}^{k+l}\lambda_i(2-\lambda_i)
\end{aligned} \tag{76}$$

where step (*a*) follows by noting $\mathbf{I}+\frac{P_A}{N_0 n_A}(\mathbf{H}_A^{CD})^{\dagger}\mathbf{H}_A^{CD} \approx \frac{P_A}{N_0 n_A}(\mathbf{H}_A^{CD})^{\dagger}\mathbf{H}_A^{CD}$ and $\mathbf{H}_A^{CD} = \mathbf{D}_{A;2,2}\mathbf{R}_{A;2,2}$, $m\in\{A,B\}$, and step (*b*) utilizes the definitions in (19a) and (26). Moreover, letting $w_A = w_B = 1$ in (42), we obtain the sum-rate of the PNC spatial streams as

$$R_A^{PNC}+R_B^{PNC} = \frac{1}{2}\sum_{m\in\{A,B\}}\left(\log\left|\frac{P_m}{N_0 n_m}\mathbf{R}_{m;1,1}\mathbf{R}_{m;1,1}^{\dagger}\right| + \log\left|\tilde{\mathbf{D}}_{m;1,1}\tilde{\mathbf{D}}_{m;1,1}^{\dagger}\right|\right). \tag{77}$$

From (44), $\mathbf{p}_i$ is the angular bisection of $\mathbf{e}_{A;i}$ and $\mathbf{e}_{B;i}$, or equivalently, $\mathbf{p}_i = [1,0]^T$, for the sum-rate case of $w_A = w_B = 1$. Then, using the definition in (33), we obtain

$$\log\left|\tilde{\mathbf{D}}_{m;1,1}\tilde{\mathbf{D}}_{m;1,1}^{\dagger}\right| = \sum_{i=k+1}^{k+l'}\log\frac{\lambda_i}{2}. \tag{78}$$

Combining (75)-(78), we complete the proof of Theorem 3.

APPENDIX C

PROOF OF LEMMA 1

We prove by using the theory of free probability [27]. The a.e.d. of $\mathbf{U}_m\mathbf{U}_m^{\dagger}$ is given by

$$p_m(\lambda) = \eta_m\delta(\lambda-1) + (1-\eta_m)\delta(\lambda),\ m\in\{A,B\}.$$

Let X_m be a random variable with PDF $p_m(\lambda)$. Its Stieltjes transform is given by (cf., (2.40) in [26])

$$S_{X_m}(z) = E\left[\frac{1}{X_m - z}\right] = \frac{\eta_m}{1-z} - \frac{1-\eta_m}{z}.$$

Then, the inverse function of $S_{X_m}(z)$ is given by

$$S_{X_m}^{-1}(s) = \frac{-(1-s)\pm\sqrt{(1-s)^2-4s(\eta_m-1)}}{2s}.$$

Using the relation between Stieltjes transform and R-transform (cf., (2.72) in [26]), we obtain the R-transform of X_m as

$$R_{X_m}(z) = S_{X_m}^{-1}(-z) - \frac{1}{z} = \frac{z-1 \mp \sqrt{(z-1)^2 + 4\eta_m z}}{2z}.$$

From Theorem 2.64 of [26], as $\mathbf{U}_A\mathbf{U}_A^\dagger$ and $\mathbf{U}_B\mathbf{U}_B^\dagger$ are asymptotically free random matrices, the R-transform of the a.e.d. of $\mathbf{U}_A\mathbf{U}_A^\dagger + \mathbf{U}_B\mathbf{U}_B^\dagger$ is given by

$$R_{AB}(z) = R_{X_A}(z) + R_{X_B}(z) = \sum_{m\in\{A,B\}} \frac{z-1 \mp \sqrt{(z-1)^2 + 4\eta_m z}}{2z}.$$

Then, the Stieltjes transform of the a.e.d. of $\mathbf{U}_A\mathbf{U}_A^\dagger + \mathbf{U}_B\mathbf{U}_B^\dagger$ satisfies

$$S_{AB}^{-1}(-z) = 1 \mp \sum_{m\in\{A,B\}} \frac{\sqrt{(z-1)^2 + 4\eta_m z}}{2z}.$$

Letting $y = S_{AB}^{-1}(-z)$, we obtain

$$\sum_{m\in\{A,B\}} \sqrt{(z-1)^2 + 4\eta_m z} = \mp 2z(y-1).$$

Multiplying $\sqrt{(z-1)^2 + 4\eta_A z} - \sqrt{(z-1)^2 + 4\eta_B z}$ on both sides, we have

$$\sqrt{(z-1)^2 + 4\eta_A z} - \sqrt{(z-1)^2 + 4\eta_B z} = \mp \frac{2(\eta_A - \eta_B)}{y-1}.$$

Adding the above two equations and taking the square, we further obtain

$$(z-1)^2 + 4\eta_A z = \left(z(y-1) + \frac{\eta_A - \eta_B}{y-1}\right)^2.$$

Solving z, we obtain

$$S_{AB}(z) = -\frac{1-\eta_A-\eta_B \mp \sqrt{(1-\eta_A-\eta_B)^2 + (2z-z^2)\left(\left(\frac{\eta_A-\eta_B}{z-1}\right)^2 - 1\right)}}{2z-z^2}.$$

From (2.45) in [26], the a.e.d. of $\mathbf{U}_A\mathbf{U}_A^\dagger + \mathbf{U}_B\mathbf{U}_B^\dagger$ is given by

$$\mathcal{F}(\lambda) = \lim_{\omega\to 0^+} \frac{1}{\pi} \operatorname{Im}\left[S_{AB}(\lambda + j\omega)\right].$$

Thus, for $0 < \lambda < 1$ and $1 < \lambda < 2$, we obtain

$$\mathcal{F}(\lambda) = \frac{1}{\pi} \operatorname{Im}\left[\frac{\sqrt{(1-\eta_A-\eta_B)^2 + \left(2\lambda-\lambda^2\right)\left(\left(\frac{\eta_A-\eta_B}{\lambda-1}\right)^2 - 1\right)}}{2\lambda-\lambda^2}\right]. \tag{79}$$

In addition, for a randomly generated pair of $\mathbf{U}_A$ and $\mathbf{U}_B$, there are $n_A + n_B - n_R$ orthogonal eigenvectors for $\lambda_i = 2$, $|n_A - n_B|$ orthogonal eigenvectors for $\lambda_i = 1$, and $n_R - n_A - n_B$ orthogonal eigenvectors for $\lambda_i = 0$. Thus, as n_R tends to infinity, the PDF $\mathcal{F}(\lambda)$ at $\lambda = 2$ is given by $[\eta_A + \eta_B - 1]^+ \delta(\lambda - 2)$; that at $\lambda = 1$ is given by $|\eta_A - \eta_B| \delta(\lambda - 1)$; and that at $\lambda = 0$ is given by $[1 - \eta_A - \eta_B]^+ \delta(\lambda)$. This concludes the proof of the lemma.

ACKNOWLEDGMENT

The work of Xiaojun Yuan was partially supported by a grant from the University Grants Committee (Project No. AoE/E-02/08) of the Hong Kong Special Administrative Region, China. The work of Tao Yang was supported by CSIRO OCE Postdoctoral Fellowships. It is also supported under the Australian Government's Australian Space Research Program.

REFERENCES

[1] R. Ahlswede, N. Cai, S.-Y. R. Li, and R. W. Yeung, "Network information flow," *IEEE Trans. Inf. Theory*, vol. 46, pp. 1204–1216, Oct. 2000.

[2] S. Zhang, S. Liew, and P. P. Lam, "Hot topic: physical-layer network coding," in Proc. 12th Annual International Conf. Mobile Computing Networking (ACM MobiCom'06), Sept. 2006, pp. 358-365.

[3] B. Nazer and M. Gastpar, "The case for structured random codes in network communication theorems," *ITW 2007*, Lake Tahoe, California, Sept., 2007.

[4] P. Popovski and H. Yomo, "Physical network coding in two-way wireless relay channels," *IEEE ICC*, Glasgow, Scotland, June 2007.

[5] W. Nam, S. Chung, Y. H. Lee, "Capacity of the Gaussian two-way relay channel to within 1/2 bit", *IEEE Trans. Inf. Theory*, vol. 56, no. 11, pp. 5488-5494, Nov. 2010.

[6] M. P. Wilson, K. Narayanan, H. D. Pfister and A. Sprintson, "Joint physical layer coding and network coding for bidirectional relaying", *IEEE Trans. Inf. Theory*, vol. 56, no. 11, pp. 5641-5654, Nov. 2010.

[7] G. Foschini, "Layered space-time architecture for wireless communication in a fading environment when using multi-element antennas," *Bell Labs Technical Journal*, Autumn 1996, pp. 41-59.

[8] S. Katti, S. Gollakota, and D. Katabi, "Embracing wireless interference: Analog network coding", *ACM SIGCOMM'07*.

[9] R. Zhang, Y.-C. Liang, C. C. Chai, and S. Cui, "Optimal beamforming for two-way multi-antenna relay channel with analogue network coding," *IEEE J. Select. Area. Comm.*, Vol. 27, No. 5, pp. 699-712, June 2009.

[10] S. Xu and Y. Hua, "Source-relay optimization for a two-way MIMO relay system", *Proc. IEEE ICCASP 2010*, pp. 3038-3041.

[11] M. Aleksic, P. Razaghi, and W. Yu, "Capacity of a class of modulo-sum relay channels," *IEEE Trans. Inf. Theory*, vol. 55, pp. 921–930, March 2009.

[12] S. H. Lim, Y.-H. Kim, A. El Gamal, and S.-Y. Chung, “Noisy network coding,” *IEEE Trans. Inf. Theory*, vol. 57, pp. 3132–3152, May 2011.

[13] G. Kramer, M. Gastpar, and P. Gupta, “Cooperative strategies and capacity theorems for relay networks,” *IEEE Trans. Inf. Theory*, vol. 51, pp. 3037–3063, September 2005.

[14] A. El Gamal, N. Hassanpour, and J. Mammen, “Relay networks with delays,” *IEEE Trans. Inf. Theory*, vol. 53, pp. 3413–3431, October 2007.

[15] D. Gunduz, A. Goldsmith and H. V. Poor, “MIMO two-way relay channel: diversity-multiplexing tradeoff analysis”, *Asilomar 2008*.

[16] H. J. Yang, J. Chun and A. Paulraj, “Asymptotic capacity of the separated MIMO two-way relay channel”, *IEEE Trans. Inf. Theory*, vol. 57, no. 11, pp. 7542-7554, Nov. 2011.

[17] T. Yang, X. Yuan, P. Li, I. B. Collings and J. Yuan., “Eigen-direction alignment based physical-layer network coding for MIMO two-way relay channels,” *IEEE Trans. Comm.*, submitted, 2012. (Available at http://arxiv.org/abs/1201.2471)

[18] A. Khina, Y. Kochman, U. Erez, “Physical-layer MIMO relaying,” in *Proc. ISIT’11*.

[19] B. Nazer and M. Gasper, “Compute-and-forward: Harnessing interference through structured codes,” *IEEE Trans. Inf. Theory*, vol. 57, pp. 6463-6486, Oct. 2011.

[20] 3GPP, “Overview of 3GPP Release 10,” Release 10 V0.1.1 (2011-6), June 2011. (Available at http://www.3gpp.org/Release-10)

[21] IEEE, “IEEE Standard for Local and metropolitan area networks Part 16: Air Interface for Broadband Wireless Access Systems Amendment 3: Advanced Air Interface,” IEEE Std 802.16m-2011, May 2011. (Available at http://www.ieee802.org/16/published.html)

[22] U. Erez and R. Zamir, “Achieving 1/2log(1 + SNR) on the AWGN channel with lattice encoding and decoding,” *IEEE Trans. Inf. Theory*, vol. 50, pp. 2293-2314, Oct. 2004.

[23] G. H. Golub and C. F. V. Loan, *Matrix Computation*, 3rd ed. Baltimore, MD: The Johns Hopkins University Press, 1997.

[24] T. M. Cover, and J. A. Thomas, *Elements of Information Theory*, Wiley, New York, 1991.

[25] S. Boyd and L. Vandenberghe, *Convex Optimization*, Cambridge University Press, 2004.

[26] A. Tulino and S. Verdu, *Random Matrix Theory and Wireless Communications*, Now Publishers Inc, 2004, ISBN: 193301900X.

[27] D. Voiculescu, “The analogues of entropy and of Fisher’s information measure in free probability theory, I,” *Communications in Math. Physics*, vol. 155, pp. 71–92, July 1993.

[28] D. Tse and P. Visanath, *Fundamentals of Wireless Communications*, Cambridge University Press, 2006.

[29] R. A. Horn and C. R. Johnson, *Matrix Analysis*, *Cambridge Unversity Press*, 1990.

[30] W. Yu, W. Rhee, S. Boyd, and J. Cioffi, “Iterative waterfilling for Gaussian vector multiple access channels,” *IEEE Trans. Inf. Theory*, vol. 50, no. 1, 145-151, Jan. 2004.

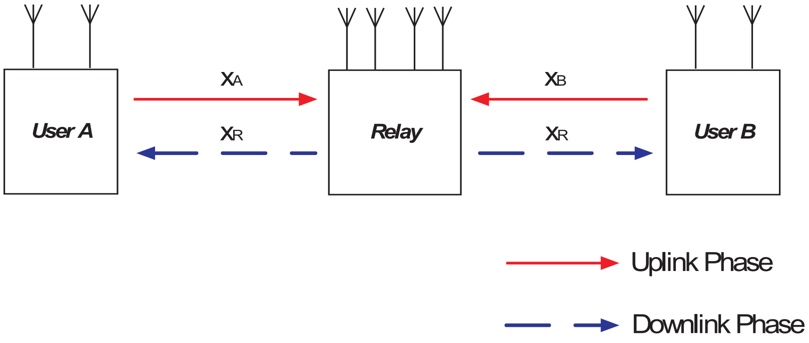

Fig. 1. Configuration of a MIMO TWRC.

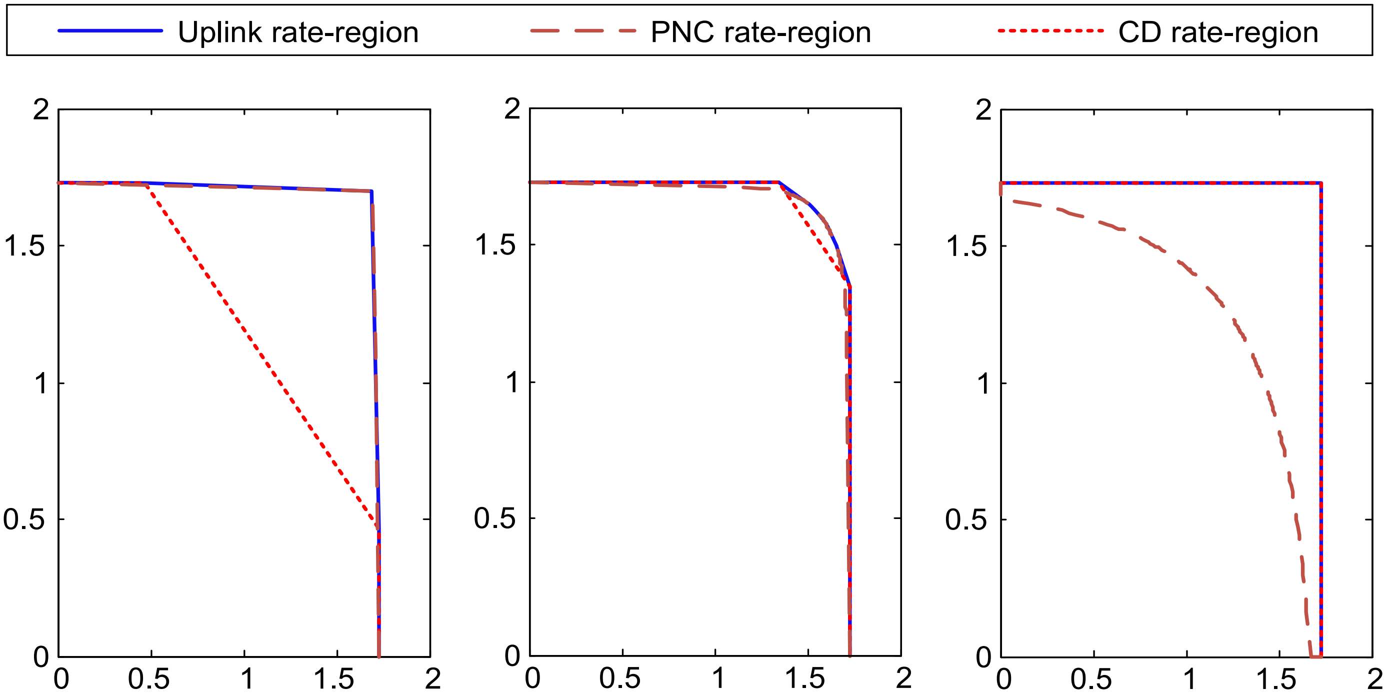

(a) $\theta = 1°$ (b) $\theta = 45°$ (c) $\theta = 89°$

Fig. 2. The uplink rate-regions of the TWRCs with single-antenna users. $\mathbf{h}_A = [1, 0]^T$ and $\mathbf{h}_B = [\cos\theta, \sin\theta]^T$. Channel SNR = $1/N_0$ = 10 dB. The horizontal axises represent the rate of user A; the vertical axises represent the rate of user B; the unit is *bit per channel use*.

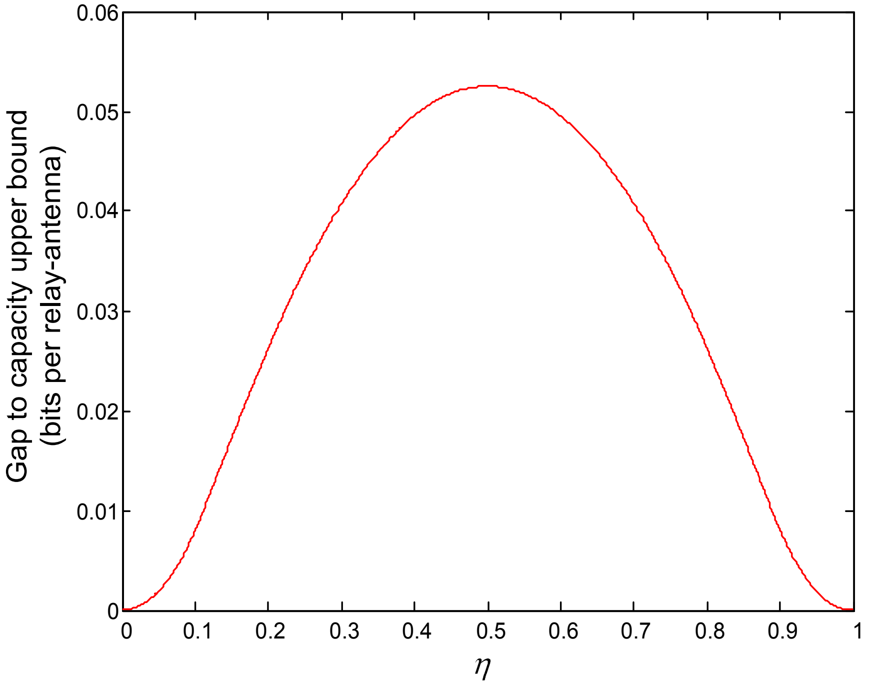

Fig. 3. The function of the average normalized gap r^{SD} in (53) against η.

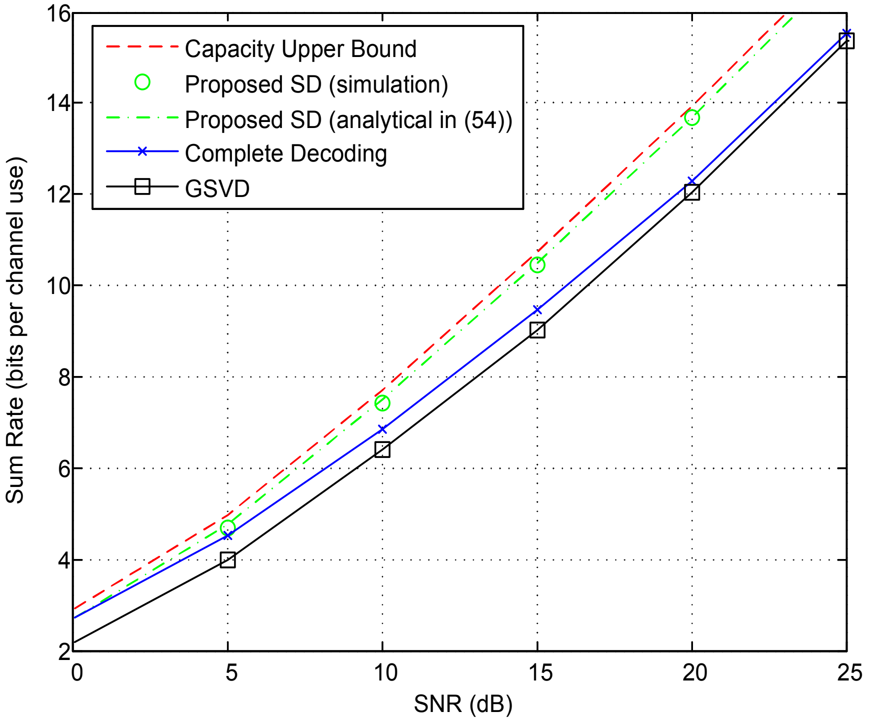

Fig. 4. Average achievable sum-rates of various schemes for the Rayleigh fading MIMO TWRC with $n_A = n_B = 2$ and $n_R = 4$.

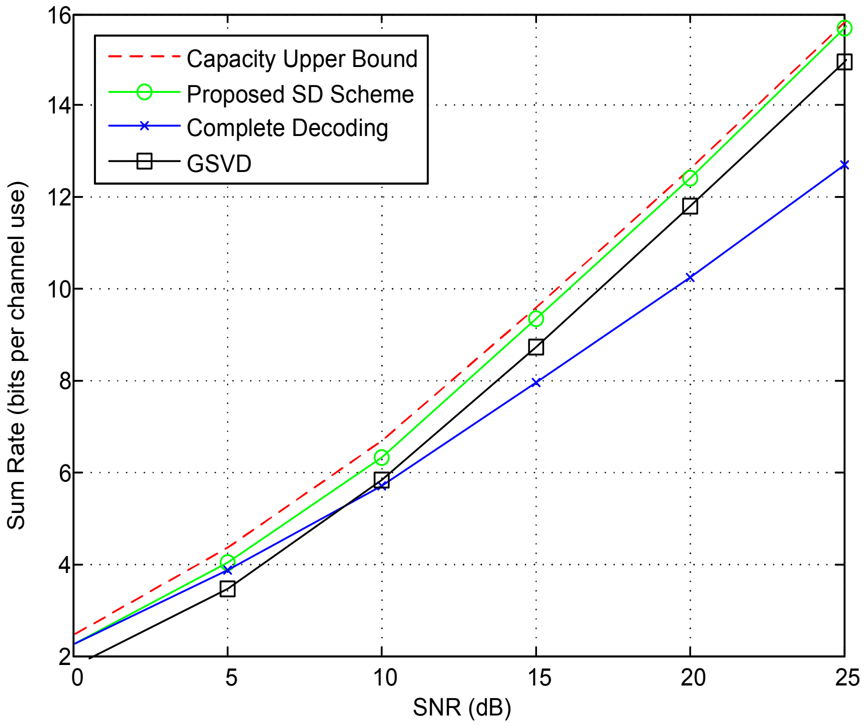

Fig. 5. Average achievable sum-rates of various schemes for the Rayleigh fading MIMO TWRC with $n_A = n_B = 2$ and $n_R = 3$.

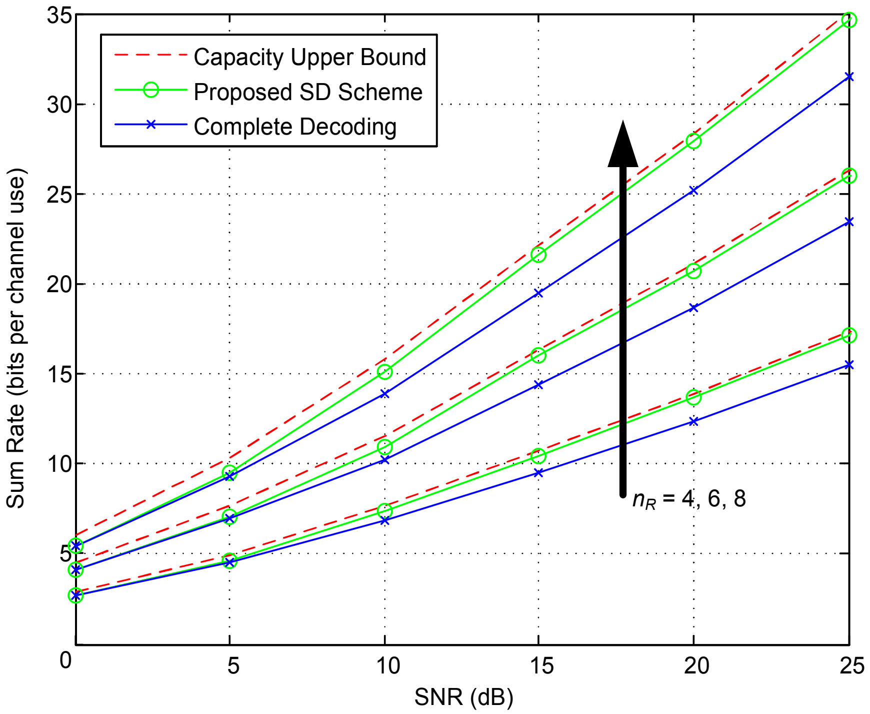

Fig. 6. Scaling effect of the average sum-rates of various schemes for the Rayleigh fading MIMO TWRCs with $\eta_A = \eta_B = 1/2$.

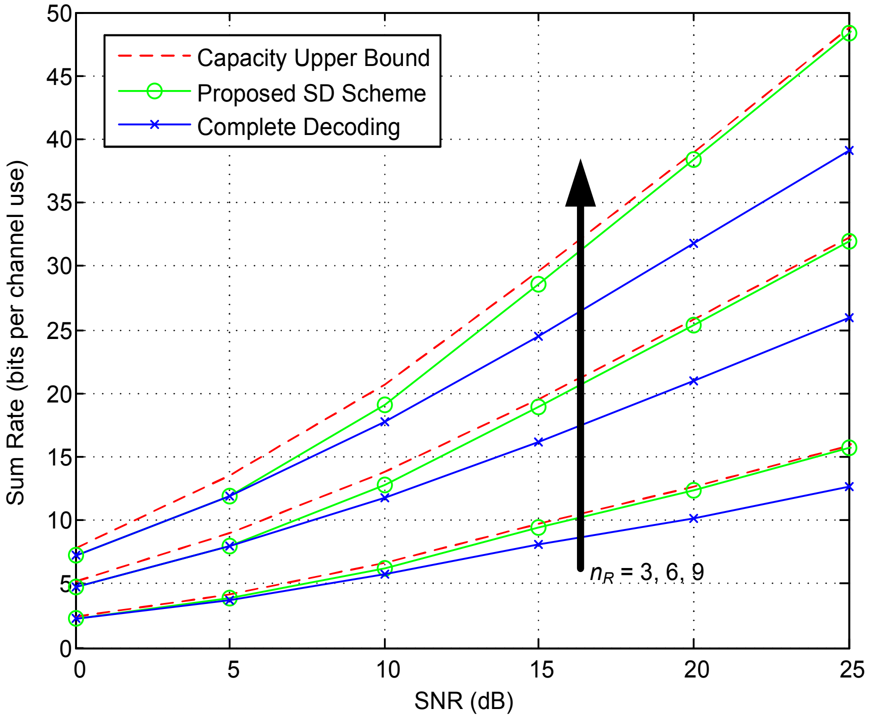

Fig. 7. Scaling effect of the average sum-rates of various schemes for the Rayleigh fading MIMO TWRCs with $\eta_A = \eta_B = 2/3$.

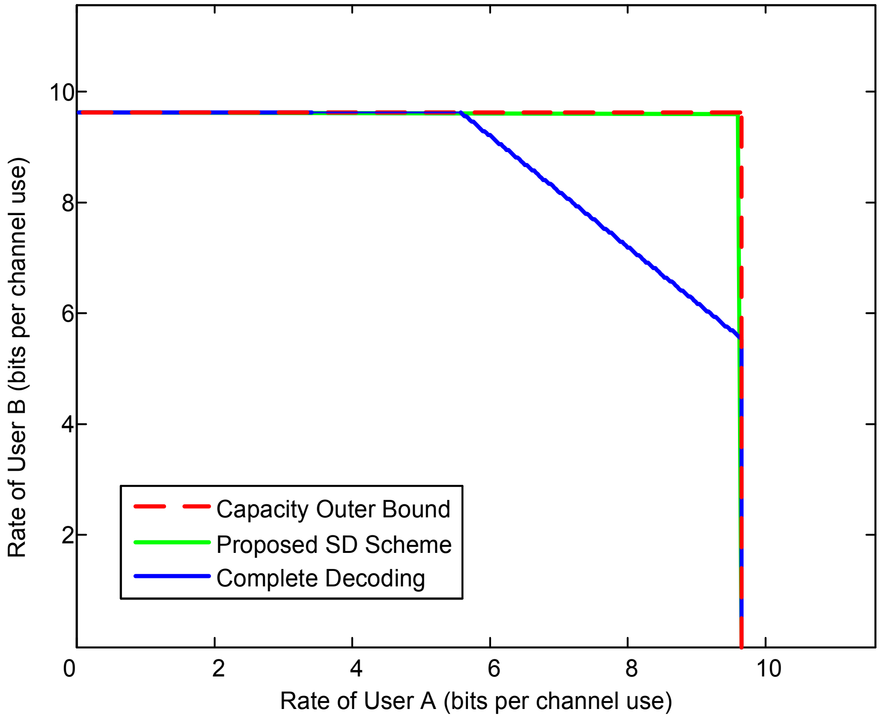

Fig. 8. Average achievable rate-regions for the Rayleigh fading MIMO TWRC with $n_A = n_B = 2$ and $n_R = 3$. The average SNRs for all the channel links are set to 30 dB.